NATIONAL ADVISORY COMMITTEE FOR AERONAUTICS

TECHNICAL NOTE 2521

LAMINAR BOUNDARY LAYER ON A CIRCULAR CONE IN SUPERSONIC FLOW AT A SMALL ANGLE OF ATTACK

By Franklin K. Moore

Lewis Flight Propulsion Laboratory
Cleveland, Ohio

Washington

October 1951

NATIONAL ADVISORY COMMITTEE FOR AERONAUTICS

Technical Note 2521

LAMINAR BOUNDARY LAYER ON A CIRCULAR CONE IN SUPERSONIC FLOW AT A SMALL ANGLE OF ATTACK

By Franklin K. Moore .

SUMMARY

The laminar boundary layer on a circular cone at angle of attack to a supersonic stream is analyzed. A solution for the outer nonviscous flow, as obtained by a method of perturbation in angle of attack, is available and is presumed to govern the development of the boundary layer, subject to certain restrictions and corrections.

In the limit of vanishing cone angle, the boundary-layer equations reduce to those for the flow about a yawed infinite cylinder in compressible flow, but may not be solved in the simple manner appropriate to incompressible flow.

For small angle of attack, the boundary-layer quantities are considered to differ only slightly from the corresponding quantities in the known flow at zero angle of attack. The system of equations resulting from this assumption are solved to yield the effect of small angle of attack on the velocity profiles, skin friction, boundary-layer thickness, and the forces and moment on the cone, or, more precisely, the rates of change of these quantities with angle of attack, evaluated at zero angle of attack.

All boundary-layer quantities show parabolic similarity in meridional planes. Circumferentially, the boundary-layer thickness associated with the profile of the circumferential velocity component is constant, and the profile itself exhibits no tendency to separate; whereas the profile of the meridional component undergoes changes caused by angle of attack which show the expected effects of secondary flow in the boundary layer.

INTRODUCTION

The flow around bodies of revolution at positive angles of attack is characterized by a draining of the boundary layer from the underside

to the top, causing the formation of "lobes" of low-energy air near the top of the body. For sufficiently large angles of attack, separation of the cross-flow may result in a transversely shed Kármán vortex street. Under these circumstances, large viscous contributions to lift, drag, and pitching moment on the body may be expected. Of course, viscous lift, drag, and moment are expected at any angle of attack, whether or not cross-flow separation occurs.

The present investigation, conducted at the NACA Lewis laboratory, is concerned with a special case, namely, the laminar boundary layer which develops on a right circular cone at a small angle of attack to the incident supersonic flow. Solutions of the laminar boundary-layer equations are sought in order to describe the viscous effects due to angle of attack, and particularly those contributing to lift, drag, and pitching moment.

As is customary, it will be assumed that the nonviscous solution for the supersonic flow about a cone at angle of attack is valid, except in a thin viscous layer enveloping the cone surface. The nonviscous flow is conical in the Busemann sense; that is, physical quantities are constant along rays from the apex. According to the analysis of Stone (reference 1), the flow quantities may be considered to be the sums of the corresponding quantities of zero angle of attack and small increments linear in angle of attack. This theory forms the basis for the extensive tables prepared at Massachusetts Institute of Technology under the supervision of Kopal (references 2 and 3). The tables of references 2 and 3 will be used in the present report. In reference 4, Ferri criticizes the Stone-Kopal treatment of the entropy gradients near the body and proposes a correction to the tables of reference 3. The applicability of this correction will be discussed in a subsequent section.

The boundary layer itself is to be treated in the manner of reference 5, wherein it is shown that "conical" bodies in supersonic flow have boundary layers which develop parabolically along generators of the surface. This boundary-layer development is a consequence of the fact that the outer nonviscous flows over such bodies have vanishing velocity and pressure gradients along rays from the apex.

The special case of a right circular cone at zero angle of attack has been solved by Hantsche and Wendt in reference 6 and by Mangler in an unavailable report. These solutions give a boundary layer which thickens parabolically along cone generators, and provide a formula for viscous drag which is valid also for small angle of attack, as will be shown subsequently.

A comparison is made herein between the present analysis and the hypothesis, which has been discussed by Allen (reference 7) and Van Dyke (reference 8), that the viscous cross flow associated with the flight of bodies of revolution at angle of attack be regarded as essentially

that which would occur in the case of an infinite circular cylinder at yaw with respect to the incident stream, a flow which has been analyzed by Prandtl, by R. T. Jones, and by Sears (reference 9). The attractiveness of this hypothesis lies in the fact that, for the yawed infinite cylinder in incompressible flow, the cross flow may be obtained from two-dimensional theory without regard to the spanwise component. In reference 5, however, it is pointed out that the chordwise velocity component does depend to some degree on the spanwise component in the case of compressible flow about a yawed infinite cylinder. Whether or not this consideration is of practical importance has not yet been ascertained.

NONVISCOUS FLOW ABOUT CONE AT ANGLE OF ATTACK

In order to treat the boundary layer on a cone at angle of attack, it is necessary first to describe the nonviscous flow about the body, particularly the velocity components and properties of state which would be predicted at the surface. Figure 1 shows the coordinate system and other notation to be used. The distance x is measured along generators of the cone; y, normal to the cone surface; and φ, circumferentially around the cone. The velocity components u, v, and w are in the x-, y-, and φ-direction, respectively. The cone has a semivertex angle of θ and is at an angle of attack α. The subscript 0 denotes conditions in the undisturbed stream, and subscript 1 denotes evaluation of the nonviscous flow at the cone surface, or, alternatively, at the outer edge of the boundary layer. The symbol notation used herein appears in appendix A.

Since the present report is concerned with small angles of attack, and correspondingly small departures of the entire flow from that occurring at zero angle of attack, it will be convenient to refer all physical quantities to this basic nonviscous flow. Thus, denoting by bars the properties at zero angle of attack, evaluated at the cone surface, the following symbols on the left will hereinafter be identified with the dimensionless groups on the right:

$$\left.\begin{aligned} u, w &\sim u/\bar{u},\ w/\bar{u} \\ \rho &\sim \rho/\bar{\rho} \\ T &\sim 2C_p T/\bar{u}^2 \\ p &\sim p/\bar{\rho}\bar{u}^2 \end{aligned}\right\} \qquad (1)$$

Thus, for example, $\bar{T} \sim 2C_p\bar{T}/\bar{u}^2 = \left(\frac{\gamma-1}{2}\bar{M}^2\right)^{-1}$

On the surface of the cone, the theory for small angle of attack used in reference 3 yields results which may be written in the following form:

$$\left.\begin{aligned} u_1 &= 1 - \alpha A_1 \cos\varphi \\ w_1 &= \alpha A_2 \sin\varphi \\ p/\bar{p} &= 1 + \alpha A_3 \cos\varphi \\ \rho_1 &= 1 + \alpha A_4 \cos\varphi \end{aligned}\right\} \qquad (2)$$

where the A's correspond as follows to the quantities (evaluated at the cone surface) tabulated in reference 3 and do not themselves depend on α:

$$\left.\begin{aligned} A_1 &\sim -x/\bar{u} \\ A_2 &\sim -z/\bar{u} - 2x/(\bar{u}\sin\Theta) \\ A_3 &\sim \eta/\bar{p} \\ A_4 &\sim \xi/\bar{\rho} \end{aligned}\right\} \qquad (3)$$

The barred ($\alpha = 0$) quantities are tabulated in reference 2. The quantities on the right side of equations (3) are in the symbol notation of reference 3.

The relations (2) provide the boundary conditions to be imposed on the viscous flow at the outer edge of the boundary layer.

If the definitions used in reference 3 were to be followed strictly, then $A_2 \sim z/\bar{u}$. The corresponding relation in set (3) is written differently in order to compensate for a systematic error in the tables. This error, confirmed by Professor Kopal in a letter to the Lewis laboratory, consists in the use of the wrong sign for the quantity C appearing in equation (34) of reference 3. Only the values of z (and hence A_2) are affected. Since C refers to the deviation of entropy in the flow due to the cone thickness, the correction described is of little consequence for small cone vertex angles, but is substantial for the larger vertex angles.

In reference 4, it is pointed out that the relations (2) imply that the change in entropy at the cone surface due to angle of attack varies circumferentially around the cone as $\cos\varphi$, whereas physical reasoning

indicates that at the cone surface the entropy should be constant except for a singularity at $\varphi = \pi$. This difficulty arises because the method of linearization in angle of attack used in reference 3 is improper near the cone surface. In reference 4 it is concluded that the tables of reference 3 are correct, except in a "vortical layer" of an angular thickness of order α^2 (infinitesimally thin in the linear approximation) across which there are a sudden change in entropy of order α and corresponding changes in other flow quantities, such as velocity and temperature, but not pressure. The "vortical layer" is a transition region in which the form of the entropy variation must change from the type $\cos \varphi$ away from the surface to constant at the cone surface.

The corrections to the tables of reference 3 required to take account of this effect are not used in the present report; that is, the boundary layer will be considered as governed by the flow external to the layer alluded to in reference 4. The following argument is presented to justify this point of view: The reason for considering the entropy constant at the surface is, briefly, that the fluid particles nearest the surface must all have passed through the conical bow shock wave in the vicinity of $\varphi = 0$ and, once past the shock, will conserve their entropy at the value appropriate to the strength of the shock at $\varphi = 0$. Thus, the sharp normal gradients near the surface (discussed in reference 4) may be considered to exist by reason of the conservation of entropy along the streamlines nearest the wall. If the boundary layer is much thicker than the "vortical layer" (α^2), the boundary layer will immediately entrain most of the fluid in the vicinity of $\varphi = 0$, which would otherwise proceed along the surface to form the base of the vortical layer. The properties of the entrained particles will then diffuse through the boundary layer by the action of viscosity, entropy will no longer be conserved next to the wall, and the constraint giving rise to the vortical layer will be removed.

Thus, it is reasonable to suppose that viscous diffusion in the boundary layer will prevent the formation of the vortical layer described in reference 4, and that the boundary layer will be governed at its outer edge by the flow described in reference 3 (equations (2)), provided that the boundary layer is much thicker than would be the vortical layer. If the reverse were true, the boundary layer would certainly be governed by conditions more nearly appropriate to the base of the vortical layer. The criterion for entrainment and diffusion of the vortical layer would be

$$\delta >> x\alpha^2$$

where δ is the boundary-layer thickness. As a rough approximation (reference 6),

$$\delta \approx (x/R)^{\frac{1}{2}}$$

where R is Reynolds number per unit length. Thus, the criterion is

$$R_x \ll \alpha^{-4}$$

Since the present analysis will concern only small angles of attack, and, strictly speaking, will be precise only in the limit $\alpha \to 0$, consistency requires that the inequality $R_x \ll \alpha^{-4}$ be presumed applicable. Of course, since the vortical layer is associated with entropy variation, this question is of less importance for smaller cone vertex angles.

LAMINAR BOUNDARY LAYER ON CONE AT ANGLE OF ATTACK

Differential Boundary-Layer Equations and Boundary Conditions

In reference 5 it is shown that the differential equations for the compressible laminar boundary layer on a conical body in supersonic flow may be written:

$$\left[f + \frac{1}{3}\frac{p'(\zeta)}{p} g + \frac{2}{3} g_\zeta\right] f_{\lambda\lambda} - \frac{2}{3} g_\lambda f_{\lambda\zeta} + \frac{2}{3} (g_\lambda)^2 + 2f_{\lambda\lambda\lambda} = 0 \quad (4a)$$

$$\left[f + \frac{1}{3}\frac{p'(\zeta)}{p} g + \frac{2}{3} g_\zeta\right] g_{\lambda\lambda} - \frac{2}{3} g_\lambda g_{\lambda\zeta} - \frac{2}{3} g_\lambda f_\lambda - \frac{2}{3}\frac{p'(\zeta)}{\rho} + 2g_{\lambda\lambda\lambda} = 0 \quad (4b)$$

$$T + (f_\lambda)^2 + (g_\lambda)^2 = T_1 + u_1^2 + w_1^2 \quad (4c)$$

$$p = \frac{\gamma - 1}{2\gamma} \rho T \quad (4d)$$

Equations (4a) and (4b) are momentum equations, equation (4c) is an energy balance, and equation (4d) is the equation of state. The functions $f(\lambda,\zeta)$ and $g(\lambda,\zeta)$ are related to the two-component vector potential discussed in reference 5 and are defined according to the relations

$$\left.\begin{aligned} u &= f_\lambda \\ w &= g_\lambda \end{aligned}\right\} \quad (5)$$

and in a manner such as to satisfy the continuity equation identically.

These equations embody the following physical assumptions, in addition to those arising from the concept of a thin boundary layer (for example, that pressure does not vary across the boundary layer):

(a) Prandtl number of 1 and constant specific heats

(b) No heat transfer through the body surface

(c) Validity of the temperature-viscosity relation

$$\frac{\mu}{\bar{\mu}} = C\,\frac{T}{\bar{T}} \tag{6a}$$

where C is defined as follows, in order to match relation (6a) to the Sutherland formula at the cone surface (denoted by subscript w):

$$C \equiv \left(\frac{T_w}{\bar{T}}\right)^{\frac{1}{2}} \frac{1 + S/\bar{T}}{T_w/\bar{T} + S/\bar{T}} \tag{6b}$$

the quantity S being taken equal to $(216^\circ\ R)\ 2C_p/\bar{u}^2$. This temperature-viscosity relation as applied to flow over a flat plate is discussed by Chapman and Rubesin in reference 10. Since the case of Prandtl number of 1 and no heat transfer is under consideration, T_w may be taken equal to the stream stagnation temperature (equation (4c)).

The coordinates x and y (fig. 1) have been made dimensionless by referring them to the length $C\,\frac{\bar{\mu}}{\bar{\rho}\bar{u}}$. Thus, the normalizing relation

$$x,y \sim \frac{\bar{\rho}\bar{u}x}{C\bar{\mu}},\ \frac{\bar{\rho}\bar{u}y}{C\bar{\mu}} \tag{7}$$

should be added to the conventions (1) previously established.

The coordinate λ has been formed as follows:

$$\lambda \equiv \sqrt{3}\left[\left(\frac{p}{\bar{p}}\right)^{-\frac{1}{2}} \int_0^y \rho\ dy\right] x^{-\frac{1}{2}} \tag{8}$$

Equations (4) and definition (8) show that similarity of the Blasius type exists in meridional planes. Thus, for example, boundary-layer thickness

is proportional to $x^{1/2}$ and may be said to increase parabolically with x. This fact is a consequence of the vanishing pressure gradient along generators of a conical body in supersonic flow.

The variable ζ is a dimensionless coordinate which, in the case of a circular cone, may be replaced by $\varphi \sin \theta$, or by $\varphi\theta$ where $\theta \equiv \sin \theta$. Equations (4) may thus be rewritten:

$$\left[f + \frac{1}{3\theta}\frac{p'(\varphi)}{p} g + \frac{2}{3\theta} g_{\varphi}\right] f_{\lambda\lambda} - \frac{2}{3\theta} g_{\lambda} f_{\lambda\varphi} + \frac{2}{3}(g_{\lambda})^2 + 2f_{\lambda\lambda\lambda} = 0 \quad (9a)$$

$$\left[f + \frac{1}{3\theta}\frac{p'(\varphi)}{p} g + \frac{2}{3\theta} g_{\varphi}\right] g_{\lambda\lambda} - \frac{2}{3\theta} g_{\lambda} g_{\lambda\varphi} - \frac{2}{3} g_{\lambda} f_{\lambda} - \frac{2}{3\theta}\frac{p'(\varphi)}{\rho} + 2g_{\lambda\lambda\lambda} = 0 \quad (9b)$$

$$T + (f_{\lambda})^2 + (g_{\lambda})^2 = T_1 + u_1^2 + w_1^2 \quad (9c)$$

$$p = \frac{\gamma - 1}{2\gamma} \rho T \quad (9d)$$

The boundary conditions on the functions $f(\lambda,\varphi)$ and $g(\lambda,\varphi)$ are: At the outer edge of the boundary layer, the u and w velocity components should take on the corresponding nonviscous values

$$f_{\lambda}(\infty,\varphi) = u_1(\varphi) \quad (10a)$$

$$g_{\lambda}(\infty,\varphi) = w_1(\varphi) \quad (10b)$$

and at the cone surface, the u, v, and w velocities should vanish,

$$f_{\lambda}(0,\varphi) = g_{\lambda}(0,\varphi) = 0 \quad (10c)$$

$$f(0,\varphi) = g(0,\varphi) = 0 \quad (10d)$$

Equation (10d) is equivalent to the requirement that the normal velocity component v vanish at the cone surface. This boundary condition is discussed at some length in reference 5.

Simplification of Equations in Special Limiting Cases

The problem of finding solutions of equations (9) for f and g subject to boundary conditions (10) is rather difficult. Accordingly, it is desirable to investigate the manner in which the equations simplify in certain special circumstances.

Small cone angle, large angle of attack. - Symbolically, this case may be described as follows:

$$\frac{\theta}{\alpha} << 1$$

$$\alpha \text{ of order } 1$$

These assumptions would be expected to lead to the equations for the boundary layer on a yawed infinite cylinder (the compressible analog of the flow treated in reference 9). For the purpose of this discussion, it is convenient to define new variables:

$$\Lambda \equiv \frac{\lambda}{\sqrt{3\theta}} = \left[\left(\frac{p}{\bar{p}}\right)^{-\frac{1}{2}} \int_0^y \rho \, dy\right](\theta x)^{-\frac{1}{2}} \tag{11}$$

$$F \equiv f/\sqrt{3\theta}$$

$$G \equiv g/\sqrt{3\theta}$$

Equations (9) and (10) become

$$\left[3\theta F + \frac{p'(\varphi)}{p} G + 2G_\varphi\right] F_{\Lambda\Lambda} - 2G_\Lambda F_{\Lambda\varphi} + 2\theta \, (G_\Lambda)^2 + 2F_{\Lambda\Lambda\Lambda} = 0 \tag{12a}$$

$$\left[3\theta F + \frac{p'(\varphi)}{p} G + 2G_\varphi\right] G_{\Lambda\Lambda} - 2G_\Lambda G_{\Lambda\varphi} - 2\theta G_\Lambda F_\Lambda - 2\frac{p'(\varphi)}{\rho} + 2G_{\Lambda\Lambda\Lambda} = 0 \tag{12b}$$

$$\left.\begin{aligned} F_\Lambda(\infty,\varphi) &= u_1(\varphi) \\ G_\Lambda(\infty,\varphi) &= w_1(\varphi) \\ F_\Lambda(0,\varphi) &= G_\Lambda(0,\varphi) = F(0,\varphi) = G(0,\varphi) = 0 \end{aligned}\right\} \tag{13}$$

For flow about a cone at angle of attack, F and its derivatives will be presumed to be of unit order; G and its derivatives, and the derivatives of p_1, of order α (order 1, in this case). When terms of order θ are neglected, equations (12) may be written:

$$G_\Lambda F_{\Lambda\varphi} - G_\varphi F_{\Lambda\Lambda} = \frac{p'(\varphi)}{2p} G F_{\Lambda\Lambda} + F_{\Lambda\Lambda\Lambda} \tag{14a}$$

$$G_\Lambda G_{\Lambda\varphi} - G_\varphi G_{\Lambda\Lambda} = -\frac{p'(\varphi)}{\rho}\left(1 - \frac{\rho}{2p} G G_{\Lambda\Lambda}\right) + G_{\Lambda\Lambda\Lambda} \tag{14b}$$

Equations (14) are also the equations for the compressible viscous flow about a yawed infinite cylinder and, for the incompressible case, are precisely equivalent to those treated in reference 9. Inspection of definition (11) shows that similarity exists in terms of the reciprocal square root of the local radius (θx) of the cone cross section. For an infinite cylinder at yaw, this radius would be a constant. For a sufficiently slender cone at a sufficiently large angle of attack $(\theta/\alpha \ll 1)$, the hypothesis discussed in reference 7 is therefore essentially correct; namely, that at any point on the cone, the boundary layer is that which would appear for the same angle of attack on an infinite circular cylinder having a diameter equal to the cross-sectional diameter of the cone at the point under consideration.

Equations (14a) and (14b) are coupled through the density ρ, which appears in the pressure gradient term, and therefore G cannot be obtained independently of F as in the incompressible case. Compressibility enters in this way according to the stream Mach number. In reference 8, it is suggested that the important Mach number is that based on the cross velocity.

This limiting case retains the general feature of parabolic growth of the boundary layer along cone generators despite the fact that, in the limit, the configuration is that of a cylinder of infinite length.

Small angle of attack, large cone angle. - This situation may be specified as

$$\frac{\alpha}{\theta} \ll 1$$

$$\theta \text{ of order } 1$$

presumably yielding, in the limit, the equations for the boundary layer on a cone at zero angle of attack to a supersonic stream. Equations (2) show that for small angles of attack, $u_1(\varphi) \approx 1$ and $w_1(\varphi)$ and $p'(\varphi)$ are of order α. Therefore, from equations (10), $f(\lambda,\varphi)$ will be of order 1 and $g(\lambda,\varphi)$ will be of order α. With terms of order α in equations (9a), (9b), and (10) neglected, equations (9a) and (10) become

$$ff_{\lambda\lambda} + 2f_{\lambda\lambda\lambda} = 0 \tag{15a}$$

$$f_{\lambda}(\infty,\varphi) = 1 \tag{15b}$$

$$f_{\lambda}(0,\varphi) = f(0,\varphi) = 0 \tag{15c}$$

Equation (9b) drops out because all its terms are of order α or smaller. In view of the form of equations (15), f is a function only of λ, and equation (15a) may be interpreted as an ordinary differential equation.

Equations (15) govern the boundary layer on a cone at zero angle of attack to a supersonic stream and are formally identical with the equations for plane flow over a flat plate, the difference between the cone and flat plate cases appearing only through a slightly different definition of independent variable. (See, for example, reference 6 or Mangler's work.)

PERTURBATION ANALYSIS FOR SMALL ANGLE OF ATTACK

In the remainder of this report, the laminar boundary layer on a cone at angle of attack to a supersonic stream will be analyzed as a perturbation of the flow at zero angle of attack (equation (15)); that is, under the conditions

$$\frac{\alpha}{\theta} << 1$$

θ of order 1

Formulation of Perturbation Equations

With the assumption that the entire flow may be represented as the sum of the basic flow $f_0(\lambda)$ satisfying equations (15) and correction terms proportional to angle of attack, $f(\lambda,\varphi)$ and $g(\lambda,\varphi)$ may be written

$$f \equiv f_0(\lambda) - \alpha A_1 \cos \varphi f_1(\lambda) + \ldots \tag{16a}$$

$$g \equiv \alpha A_2 \sin \varphi g_1(\lambda) + \ldots \tag{16b}$$

The quantities f_0, f_1, g_1, A_1, and A_2 are presumed of order 1. The forms of the correction terms are chosen to be consistent with the relations (2) to be imposed as boundary conditions on the boundary layer at its outer edge.

The pressure gradient terms appearing in equations (9a) and (9b) may be expressed in perturbation form with the aid of equations (2), (9c), and (9d) and definitions (16): From equations (2), since pressure is presumed not to vary across the boundary layer,

$$\frac{p'(\varphi)}{\bar{p}} = -\alpha A_3 \sin \varphi \tag{17a}$$

From equations (2), (9c), and (9d),

$$\frac{1}{\rho} = \frac{\gamma-1}{2\gamma}\frac{T}{p} = \frac{\gamma-1}{2\gamma}\frac{T_1 + u_1^2 + w_1^2 - (f_\lambda)^2 - (g_\lambda)^2}{\overline{p}\,(1 + \alpha A_3 \cos\varphi)} \tag{17b}$$

Because T_1 differs from $\overline{T}$ only by a quantity of order α, equations (16) may be substituted into equation (17b) to yield, for small α,

$$\frac{\overline{p}}{\rho} = \frac{\gamma-1}{2\gamma}\left[\overline{T} + 1 - (f_0')^2\right] + \ldots$$

which may be multiplied into equation (17a) to give

$$\frac{p'(\varphi)}{\rho} = -\alpha A_3 \sin\varphi \frac{\gamma-1}{2\gamma}\left[\overline{T} + 1 - (f_0')^2\right] + \ldots \tag{17c}$$

Substituting equations (16) and (17c) into (9a) and (9b) and equating the sum of terms of unit order in equation (9a) to zero give

$$f_0 f_0'' + 2f_0''' = 0 \tag{18}$$

The sum of terms of order α in equation (9a) is next equated to zero, yielding

$$-2\left(\frac{A_2}{\theta A_1}\right)f_0''g_1 + 3f_0 f_1'' + 3f_0''f_1 + 6f_1''' = 0 \tag{19}$$

The largest terms in equation (9b) are of order α; the sum of these terms is equated to zero:

$$3f_0 g_1'' - 2f_0' g_1' + 6g_1''' = -2\frac{A_3}{\theta A_2}\frac{\gamma-1}{2\gamma}\overline{T}\left\{1 + \frac{1}{\overline{T}}\left[1 - (f_0')^2\right]\right\} \tag{20}$$

Substituting equations (16) and (2) into boundary conditions (10) and equating terms of like order in α provide the boundary conditions to which the differential equations (18), (19), and (20) are subject:

$$f_0'(\infty) = 1 \qquad f_0'(0) = f_0(0) = 0 \tag{21}$$

$$f_1'(\infty) = 1 \qquad f_1'(0) = f_1(0) = 0 \tag{22}$$

$$g_1'(\infty) = 1 \qquad g_1'(0) = g_1(0) = 0 \tag{23}$$

In view of boundary conditions (21) and (23), the relation

$$\frac{A_3}{\theta A_2}\frac{\gamma-1}{2}\bar{T} \equiv 1 \tag{24a}$$

must hold in order that equation (20) be satisfied at $\lambda = \infty$. Because of relations (1),

$$\bar{T} = \frac{2}{\gamma-1}\frac{1}{\bar{M}^2} \tag{24b}$$

where $\bar{M}$ is the Mach number at the surface of the cone when at zero angle of attack. In terms of quantities tabulated in reference 3,

$$\bar{M}^2 = \frac{2}{\gamma-1}\frac{\bar{u}^2}{1-\bar{u}^2} \tag{24c}$$

With the aid of equations (3), (24b), and (24c), it may be verified from reference 3 that equation (24a) is indeed correct. Equation (20) may therefore be written more simply as follows:

$$3f_0g_1'' - 2f_0'g_1' + 6g_1''' = -2\left\{1 + \frac{\gamma-1}{2}\bar{M}^2\left[1 - (f_0')^2\right]\right\} \tag{25}$$

To summarize, the basic flow at zero angle of attack over the cone is determined by the solution of the boundary-value problem

$$f_0f_0'' + 2f_0''' = 0 \tag{18}$$

$$f_0'(\infty) = 1 \qquad f_0'(0) = f_0(0) = 0 \tag{21}$$

The meridional velocity component u is given by the function $f_0'(\lambda)$, according to equation (5). When $f_0(\lambda)$ is known and $\bar{M}$ is specified, the circumferential velocity component due to a small angle of attack may be determined from equations (5) and (16b) and from the solution of the problem

$$3f_0g_1'' - 2f_0'g_1' + 6g_1''' = -2\left\{1 + \frac{\gamma-1}{2}\bar{M}^2\left[1 - (f_0')^2\right]\right\} \tag{25}$$

$$g_1'(\infty) = 1 \qquad g_1'(0) = g_1(0) = 0 \tag{23}$$

Then, presuming $f_0(\lambda)$ and $g_1(\lambda)$ to have been determined and the quantity $A_2/\theta A_1$ to be specified, the increment in meridional velocity

component due to a small angle of attack may be found from equations (5) and (16a) and from the solution of the problem

$$3f_0f_1'' + 3f_0''f_1 + 6f_1''' = 2\left(\frac{A_2}{\theta A_1}\right)f_0''g_1 \tag{19}$$

$$f_1'(\infty) = 1 \qquad f_1'(0) = f_1(0) = 0 \tag{22}$$

The perturbation procedure used to obtain these differential equations is, in general, subject to an important limitation which should be examined. Since all velocity components vanish at the cone surface, it is perhaps not obvious that it is proper, near the surface, to make the neglections in equations (9) necessary to arrive at equations (19) and (25). In particular, consider the term $ff_{\lambda\lambda}$ appearing in equation (9a). Substitution of equation (16a) yields

$$ff_{\lambda\lambda} = f_0f_0'' - \alpha A_1 \cos\varphi\,(f_1f_0'' + f_0f_1'') + \alpha^2 A_1^2 \cos^2\varphi\, f_1f_1'' + \cdots \tag{26a}$$

In deriving equation (19), the term involving α^2 has been neglected in comparison with the term involving α, despite the fact that both terms vanish as $\lambda\to 0$. The problem of proper neglection near the surface becomes determinate if the last two terms of expression (26a) are written as follows:

$$-\alpha A_1 \cos\varphi\,(f_1f_0'' + f_0f_1'')\left(1 - \alpha A_1 \cos\varphi\,\frac{f_1f_1''}{f_1f_0'' + f_0f_1''}\right)$$

Thus, the question is whether or not, for $\alpha \ll 1$, the following inequality holds as $\lambda\to 0$:

$$\alpha A_1 \cos\varphi\,\frac{f_1f_1''}{f_1f_0'' + f_0f_1''} \ll 1 \tag{26b}$$

or, equivalently, whether or not

$$\frac{f_1f_1''}{f_1f_0'' + f_0f_1''} \tag{26c}$$

is always of order 1 or smaller.

Boundary conditions (21) and (22) indicate that f_0 and f_1 may be represented for small λ by the following power series:

$$f_0 = \frac{1}{2!} f_0''(0)\, \lambda^2 + \frac{1}{3!} f_0'''(0)\, \lambda^3 + \cdots$$

$$f_1 = \frac{1}{2!} f_1''(0)\, \lambda^2 + \frac{1}{3!} f_1'''(0)\, \lambda^3 + \cdots$$

If $f_0''(0) \neq 0$ (as in the present problem), then, in the limit $\lambda \to 0$, quantity (26c) is equal to $\frac{1}{2} f_1''(0)/f_0''(0)$, which is presumably no larger than unit order. All the neglections made in deriving equations (19) and (25) may be justified by this sort of argument.

If, however, $f_0''(0)$ were zero and $f_1''(0)$ were not zero, expression (26c) would become infinite as $\lambda \to 0$, and inequality (26b) would not hold. The quantities $f_0''(0)$ and $f_1''(0)$ are related to the slopes at the wall of the basic and incremental velocity profiles (equation (5)), and hence are proportional to the corresponding contributions to viscous shear stress at the wall. Thus, in general, a perturbation analysis of a boundary layer will be improper near a point where the shear stress of the basic flow vanishes, that is, near a separation point.

Solution of Perturbation Equations

The boundary-value problem for f_0 (equations (18) and (21)) arises in the case of boundary-layer flow on a flat plate and has been studied thoroughly in the literature. For completeness, the values of f_0 and its derivatives, as determined by calculations made at the Lewis laboratory, are presented in table I. The results agree precisely with those presented in reference 9.

The functions $f_1(\lambda)$ and $g_1(\lambda)$ may be expressed as linear combinations of functions not depending on the parameters $\bar{M}$ or $A_2/\theta A_1$. The following representation was proposed by L. Richard Turner of the Lewis laboratory:

$$g_1(\lambda) \equiv f_0(\lambda) + \left(1 + \frac{\gamma - 1}{2} \bar{M}^2\right) h_1(\lambda) \qquad (27a)$$

$$f_1(\lambda) \equiv \left(\frac{2}{3}\frac{A_2}{\theta A_1}\right) f_0(\lambda) + \left(1 - \frac{2}{3}\frac{A_2}{\theta A_1}\right) h_2(\lambda) + 2\left(1 + \frac{\gamma-1}{2}\overline{M}^2\right)\frac{A_2}{\theta A_1} h_3(\lambda) \tag{27b}$$

The coefficients in equations (27) may be determined from the tables of reference 3. Substituting equations (27) into equations (19), (22), (23), and (25) and making use of equations (18) and (21) yield the following differential equations and boundary conditions for the functions h_1, h_2, and h_3, which can be solved once and for all, with no regard for the physical parameters of the problem:

$$3f_0h_1'' - 2f_0'h_1' + 6h_1''' = -2\left[1 - (f_0')^2\right] \tag{28a}$$

$$h_1'(\infty) = h_1'(0) = h_1(0) = 0 \tag{28b}$$

$$3f_0h_2'' + 3f_0''h_2 + 6h_2''' = 0 \tag{29a}$$

$$h_2'(\infty) = 1 \qquad h_2'(0) = h_2(0) = 0 \tag{29b}$$

$$3f_0h_3'' + 3f_0''h_3 + 6h_3''' = f_0''h_1 \tag{30a}$$

$$h_3'(\infty) = h_3'(0) = h_3(0) = 0 \tag{30b}$$

In appendix B, the computation of h_1, h_2, and h_3 is described. The results appear in table I.

Presentation and Discussion of Results

The various important boundary-layer quantities may be found from the profile functions given in equations (27). The numerical examples presented in figures 3 to 15 have been computed with the aid of the tables of references 2 and 3.

The boundary layer on a cone at angle of attack is characterized by the phenomenon of "secondary flow," which has been described by various authors. A discussion of secondary flow as it occurs on a cone at angle of attack is provided in the following paragraphs in order to facilitate interpretation of the results of the present analysis.

Since the inviscid flow about the cone at angle of attack is "conical," the pressure gradient at the outer edge of the boundary layer is entirely circumferential (equations (2)). The streamlines in the inviscid flow just outside the boundary layer (shown schematically as solid lines in fig. 2) will incline toward the direction of the pressure gradient. Since the pressure tends to be constant across the boundary layer, the fluid in the boundary layer is subject to the same pressure gradient as is the outer flow, but has less inertia with which to resist its effect, and thus it tends to follow the direction of the pressure gradient more closely than does the outer flow.

An angular divergence therefore exists between outer streamlines and boundary-layer streamlines; the divergence is greatest when the limiting streamlines at the base of the boundary layer are considered. These limiting streamlines are shown schematically as dashed lines in figure 2. The divergence ε is defined as the local angle included between the outer and limiting streamlines.

This divergence between inner and outer streamlines ("secondary flow") clearly leads to a draining away of low-energy air from the high-pressure side of the body and a corresponding concentration of low-energy air on the low-pressure side. Accordingly, if the cone is at positive angle of attack, the skin friction would be expected to be lower at the top of the cone than at the bottom, and the boundary-layer thickness would have a maximum at the top and a minimum at the bottom.

Before proceeding further, it is perhaps well to emphasize that the present analysis is valid only in the limit of vanishing angle of attack. That is, terms multiplied by α represent rates of change with angle of attack, evaluated at zero angle of attack. All results will be presented in this form. Whether or not the absolute change for a small finite angle of attack can be obtained from this theory depends on the relative magnitude of the effect so computed, rather than on the size of α, and depends further on the (unknown) second and higher derivatives of the quantity with respect to α.

Velocity profiles and streamline divergence. - From equations (5) and (16),

$$\left.\begin{aligned} w = g_\lambda &= \alpha A_2 \sin\varphi \; g_1' \\ u = f_\lambda &= f_0' - \alpha A_1 \cos\varphi \; f_1' \end{aligned}\right\} \tag{31}$$

These expressions may be divided by the values of w_1 and u_1 given in equations (2) to yield, for $\alpha \ll 1$,

$$\frac{w}{w_1} = g_1' \tag{32a}$$

$$\frac{u}{u_1} = f_0' + \alpha A_1 \cos \varphi \, (f_0' - f_1') \tag{32b}$$

or, substituting equations (27),

$$\frac{w}{w_1} = f_0' + \left(1 + \frac{\gamma-1}{2} \overline{M}^2\right) h_1' \tag{33a}$$

$$\frac{u}{u_1} = f_0' + \alpha A_1 \cos \varphi \left[\left(1 - \frac{2}{3} \frac{A_2}{\theta A_1}\right)(f_0' - h_2') - 2\left(1 + \frac{\gamma-1}{2} \overline{M}^2\right)\frac{A_2}{\theta A_1} h_3'\right] \tag{33b}$$

2286

The outer streamline is inclined to the x-direction by an angle

$$\tan^{-1} \frac{w_1}{u_1} = \tan^{-1}\left(\frac{\alpha A_2 \sin \varphi}{1 - \alpha A_1 \cos \varphi}\right) \approx \alpha A_2 \sin \varphi$$

which is obtained by use of equations (2). The limiting streamline is inclined to the x-direction by an angle

$$\tan^{-1}\left(\lim_{\lambda \to 0} \frac{w}{u}\right) \approx \alpha A_2 \sin \varphi \, \frac{g_1''(0)}{f_0''(0)}$$

which is obtained with the aid of equations (31) and L'Hospital's rule. The divergence ε is given by the difference between these two angles:

$$\varepsilon \approx a A_2 \sin \varphi \left[\frac{g_1''(0)}{f_0''(0)} - 1\right]$$

or, by use of equation (27a) and table I,

$$\varepsilon \approx \alpha(1.291) A_2 \left(1 + \frac{\gamma-1}{2} \overline{M}^2\right) \sin \varphi \tag{34}$$

This streamline deflection due to angle of attack is indicated by the quantity

$$\frac{1}{\sin \varphi}\left(\frac{\partial \varepsilon}{\partial \alpha}\right)_{\alpha=0} = (1.291)\, A_2 \left(1 + \frac{\gamma-1}{2} \bar{M}^2\right)$$

and is shown in figure 3 as a function of stream Mach number M_0 for cone semivertex angles Θ of 10°, 20°, and 30°.

The distribution through the boundary layer of the circumferential velocity w/w_1 is shown in figure 4 for cone semivertex angles Θ of 10° and 30°, and for stream Mach numbers M_0 of 2 and 4. From equation (31) and figure 4, it is evident that no "cross-flow separation" takes place, because the profiles of figure 4 (which are not of the separation type) appear at all circumferential locations, modified by the value of $\sin \varphi$, which affects only the scale of the w-profiles.

Of course, cross-flow separation would occur for large angles of attack because of the effect of an adverse circumferential pressure gradient over part of the cone surface. For very small angles of attack, separation of the cross flow would hardly be expected since the circumferential pressure gradient is always favorable (equations (2)).

The increment in meridional velocity profile due to angle of attack is indicated by the quantity

$$\frac{1}{\cos \varphi}\left[\frac{\partial}{\partial \alpha}\left(\frac{u}{u_1}\right)\right]_{\alpha=0} = A_1 \left(f_0' - f_1'\right)$$

which is shown in figure 5 for $\Theta = 10^\circ$ and 30°, and for $M_0 = 2$ and 4. For positive angle of attack, the meridional profile is correspondingly steeper on the underside and less steep on the top. This result agrees with the qualitative argument that low-energy air should drain away from beneath the body and concentrate on the top. The order of magnitude of this effect is shown in figure 6, in which the u/u_1 profiles in the plane $\varphi = 0, \pi$ for $\alpha = 2.5^\circ$ are compared with the profiles for $\alpha = 0$, when $\Theta = 10^\circ$ and $M_0 = 4$.

The relative thickening of the boundary layer at the top of the cone and thinning at the bottom might be expected to have an adverse effect on laminar stability at the top and the reverse effect on the bottom.

Skin friction. - The circumferential and meridional components of the viscous shear stress at the cone surface may be written as coefficients:

$$C_{f_\varphi} \equiv \frac{1}{\frac{1}{2}\bar{\rho}\bar{u}^2}\left(\mu \frac{\partial w}{\partial y}\right)_w$$

$$C_{f_x} \equiv \frac{1}{\frac{1}{2}\bar{\rho}\bar{u}^2}\left(\mu \frac{\partial u}{\partial y}\right)_w$$

where the quantities making up the right sides are in dimensional form. Application of equations (1) and (4) to (8) yields

$$C_{f_\varphi} = 2\sqrt{\frac{3C}{\bar{R}_x}}\left(\frac{p}{\bar{p}}\right)^{\frac{1}{2}} g_{\lambda\lambda}(0,\varphi) \tag{34a}$$

$$C_{f_x} = 2\sqrt{\frac{3C}{\bar{R}_x}}\left(\frac{p}{\bar{p}}\right)^{\frac{1}{2}} f_{\lambda\lambda}(0,\varphi) \tag{34b}$$

where $\bar{R}_x$ is a Reynolds number based on distance from the cone apex and on fluid quantities evaluated in the nonviscous flow at the surface of the cone at zero angle of attack:

$$\bar{R}_x \equiv \frac{\bar{\rho}\bar{u}\,x}{\bar{\mu}}$$

Introduction of equations (2) and (16) yields

$$C_{f_\varphi} = 2\sqrt{\frac{3C}{\bar{R}_x}}\,\alpha\, A_2 \sin\varphi\; g_1''(0)$$

$$C_{f_x} = 2\sqrt{\frac{3C}{\bar{R}_x}}\, f_0''(0)\left[1 - \alpha A_1 \cos\varphi\left(\frac{f_1''(0)}{f_0''(0)} - \frac{A_3}{2A_1}\right)\right]$$

or, using equations (27) and table I,

$$C_{f_\varphi}\sqrt{\frac{\bar{R}_x}{3C}} = \alpha A_2 \sin\varphi\left(1.522 + 0.858\,\frac{\gamma-1}{2}\,\bar{M}^2\right) \tag{35a}$$

$$C_{f_x}\sqrt{\frac{\bar{R}_x}{3C}} = 0.664\left[1 - \alpha A_1 \cos\varphi\left(1.502 - 0.525\frac{A_2}{\theta A_1} - 0.190\frac{\gamma-1}{2}\bar{M}^2\frac{A_2}{\theta A_1} - \frac{A_3}{2A_1}\right)\right] \quad (35b)$$

The meridional skin friction at zero angle of attack is obtained by setting $\alpha = 0$ in equation (35b), yielding a result equivalent to the results of Hantsche and Wendt (reference 6) and Mangler.

In figure 7, the circumferential skin friction appears as a function of stream Mach number for semivertex angles of 10°, 20°, and 30°.

Figure 8 shows the increment due to angle of attack of meridional skin friction plotted as a function of M_0 for the same cone angles. The effect of angle of attack on meridional skin friction is of the same order of magnitude as the effect on circumferential skin friction, as would be expected in view of the previous discussion of the velocity profiles. For positive angle of attack, the meridional skin friction has a maximum at $\varphi = 0$ and a minimum at $\varphi = \pi$, which is consistent with the previous qualitative discussion of secondary flow.

Boundary-layer thickness. - The boundary-layer thicknesses are expressed as the mass-flow defects ("displacement thicknesses") associated with the u and w profiles. Thus

$$\delta_\varphi \equiv \int_0^\infty \left(1 - \frac{\rho w}{\rho_1 w_1}\right)dy$$

$$\delta_x \equiv \int_0^\infty \left(1 - \frac{\rho u}{\rho_1 u_1}\right)dy$$

or, making use of equations (1), (7), and (8) and expressing δ as a Reynolds number $\bar{R}_\delta \equiv \bar{\rho}\,\bar{u}\,\delta/\bar{\mu}$,

$$\left.\begin{aligned}\bar{R}_{\delta_\varphi} &= \sqrt{\frac{\bar{C}\bar{R}_x}{3}}\left(\frac{\bar{p}}{\bar{p}}\right)^{\frac{1}{2}} \frac{\bar{\rho}}{\rho_1}\int_0^\infty \left(\frac{\rho_1}{\rho} - \frac{w}{w_1}\right) d\lambda \\ \bar{R}_{\delta_x} &= \sqrt{\frac{\bar{C}\bar{R}_x}{3}}\left(\frac{\bar{p}}{\bar{p}}\right)^{\frac{1}{2}} \frac{\bar{\rho}}{\rho_1}\int_0^\infty \left(\frac{\rho_1}{\rho} - \frac{u}{u_1}\right) d\lambda\end{aligned}\right\} \tag{36}$$

From equations (9c) and (9d),

$$\frac{\rho_1}{\rho} = 1 + \frac{\rho_1/\bar{\rho}}{p/\bar{p}} \frac{\gamma-1}{2} \bar{M}^2\left[\frac{u_1^2}{u^2} - (f_\lambda)^2\right] \tag{37}$$

Substituting equations (5) and (37) into (36),

$$\bar{R}_{\delta_\varphi} = \sqrt{\frac{\bar{C}\bar{R}_x}{3}}\left(\frac{\bar{p}}{\bar{p}}\right)^{\frac{1}{2}} \frac{\bar{\rho}}{\rho_1}\int_0^\infty \left[1 + \frac{\rho_1/\bar{\rho}}{p/\bar{p}} \frac{\gamma-1}{2} \bar{M}^2 \frac{u_1^2}{\bar{u}^2}\left(1 - \frac{u^2}{u_1^2}\right) - \frac{w}{w_1}\right] d\lambda \tag{38a}$$

$$\bar{R}_{\delta_x} = \sqrt{\frac{\bar{C}\bar{R}_x}{3}}\left(\frac{\bar{p}}{\bar{p}}\right)^{\frac{1}{2}} \frac{\bar{\rho}}{\rho_1}\int_0^\infty \left[1 + \frac{\rho_1/\bar{\rho}}{p/\bar{p}} \frac{\gamma-1}{2} \bar{M}^2 \frac{u_1^2}{\bar{u}^2}\left(1 - \frac{u^2}{u_1^2}\right) - \frac{u}{u_1}\right] d\lambda \tag{38b}$$

Introducing equations (2) and (33a), performing the indicated integrations, and making use of table I change equation (38a) to

$$\bar{R}_{\delta_\varphi}\sqrt{\frac{3}{\bar{C}\bar{R}_x}} = 0.944 + 1.608 \frac{\gamma-1}{2} \bar{M}^2 \tag{39a}$$

It would be improper to present the term of order α resulting from integration of equation (38a) since in the present approximation the ratio w/w_1 is known only to unit order (see equation (33a)). Introducing equations (2) and (33b) into equation (38b) and performing the required integrations (with the aid of equations (18), (19), and (25)) result in the following expression:

$$\bar{R}_{\delta_x}\sqrt{\frac{3}{C\bar{R}_x}} = \left(1.721 + 2.385\,\frac{\gamma-1}{2}\,\bar{M}^2\right)\left\{1 + \alpha A_1 \cos\varphi\left[\frac{A_3}{2A_1} - \frac{A_4}{A_1} + \frac{1}{1.721 + 2.385\,\frac{\gamma-1}{2}\,\bar{M}^2}\left(0.863 - 3.576\,\frac{\gamma-1}{2}\,\bar{M}^2 - \left\{0.863 + 1.469\,\frac{\gamma-1}{2}\,\bar{M}^2 + 0.385\left[\frac{\gamma-1}{2}\,\bar{M}^2\right]^2\right\}\frac{A_2}{\theta A_1} - 2.385\,\frac{\gamma-1}{2}\,\bar{M}^2\left\{\frac{A_3}{A_1} - \frac{A_4}{A_1}\right\}\right)\right]\right\} \qquad (39b)$$

The displacement thickness associated with the u-component at zero angle of attack (obtained by setting $\alpha = 0$ in equation (39b)) is shown in figure 9, as a function of M_0 for various cone angles, and is equivalent to the results of Hantsche and Wendt (reference 6) and Mangler.

The w-thickness given by equation (39a) is shown in figure 10. This thickness does not depend on φ, and hence, at any value of x, is constant around the cone.

The increment in u-thickness due to angle of attack (fig. 11) indicates thinning of the boundary layer on the high-pressure side of the cone and thickening on the low-pressure side. This effect is qualitatively consistent with the previous discussion of secondary flow in the boundary layer of a cone at angle of attack, and its order of magnitude is consistent with the corresponding results for velocity profiles and skin friction.

Forces and moments. - The inviscid solution for flow about the cone at an angle of attack provides the forces and moments due to the action of normal pressure forces, which may be evaluated using the tables of references 2 and 3. In order to obtain the total force and moments, the forces and moments due to viscous shear at the surface must be added to the corresponding pressure forces and moments. Lift and drag are measured normal and parallel, respectively, to the stream direction. Pitching moment is measured about the cone apex, positive in the sense shown in figure 12. All quantities appearing in the following formulas are in dimensional form.

(a) Viscous drag: Written in coefficient form, the drag due to skin friction at the surface is

$$C_{D_v} \equiv \frac{D_v}{\frac{1}{2}\rho_0 u_0^2 A} = \frac{1}{A}\frac{\bar{\rho}\bar{u}^2}{\rho_0 u_0^2}\int_0^x dx \int_0^{2\pi} C_{f_x}\,\theta\sqrt{1-\theta^2}\,x\,d\varphi$$

where D_v is the viscous drag and A is the cone surface area. Using equation (35b) yields

$$C_{D_v} = 0.885\sqrt{\frac{3C}{\bar{R}_x}}\frac{\bar{p}}{p_0}\frac{\bar{M}^2}{M_0^2}\sqrt{1-\theta^2} \qquad (40)$$

This expression gives the drag at zero angle of attack. The correction due to angle of attack is of order α^2, and hence is neglected in the present linear analysis. The drag coefficient (equation (40)), which is equivalent to the results obtained by Hantsche and Wendt (reference 6) and Mangler, is shown in figure 13 as a function of M_0 for various values of θ.

(b) Viscous lift: The lift due to circumferential skin friction is

$$C_{L_v} \equiv \frac{L_v}{\frac{1}{2}\rho_0 u_0^2 A} = -\alpha\, C_{D_v} + \frac{1}{A}\frac{\bar{\rho}\bar{u}^2}{\rho_0 u_0^2}\int_0^x dx \int_0^{2\pi} C_{f_\varphi}\,\theta x \sin\varphi\; d\varphi$$

where L_v is the viscous lift. Using equation (35a),

$$C_{L_v} = \alpha\left[-C_{D_v} + \left(1.015 + 0.572\,\frac{\gamma-1}{2}\,\bar{M}^2\right)A_2\frac{\bar{p}}{p_0}\frac{\bar{M}^2}{M_0^2}\sqrt{\frac{3C}{\bar{R}_x}}\right] \qquad (41)$$

The lift coefficient is shown in figure 14 as a function of M_0 for various values of θ. Except for quite low Reynolds numbers, the laminar viscous lift is small compared with the pressure lift. The pressure lift coefficient is of order α, whereas for a Reynolds number based on slant height of 300,000, the viscous lift coefficient on a 10° cone at $M_0 = 4$ is only of the order of $0.01\,\alpha$.

2296

(c) Viscous pitching moment: By use of equation (35a), the moment due to circumferential skin friction may be found:

$$C_{m_v} \equiv \frac{m_v}{\frac{1}{2}\rho_0 u_0^2 \, Ax} = -\alpha\left(0.609 + 0.343\,\frac{\gamma-1}{2}\,\bar{M}^2\right)A_2\,\frac{\bar{p}}{p_0}\,\frac{\bar{M}^2}{M_0^2}\sqrt{1-\theta^2}\sqrt{\frac{3C}{\bar{R}_x}} \tag{42}$$

where m_v is the viscous pitching moment about the apex. The moment is shown in figure 15 as a function of M_0 for several cone angles.

CONCLUSIONS

For small angles of attack, the outer nonviscous flow about a cone at angle of attack to a supersonic stream has previously been treated by a perturbation theory, which may be used to describe the outer flow governing the development of the laminar boundary layer on the cone surface, provided that no account need be taken of the "vortical layer" recently discussed by Ferri.

This vortical layer is a region in the nonviscous flow field near the surface of the cone across which there are large gradients of entropy and velocity, and is said to have an angular thickness of the order of the square of the angle of attack. If the boundary layer is much thicker than this, then presumably viscous diffusion disperses the vortical layer, which then may be neglected.

Since the outer nonviscous flow is "conical," use may be made of previously derived differential equations for a boundary layer governed by an outer flow with conical symmetry. These equations imply a solution having parabolic similarity in meridional planes. Assuming a Prandtl number of 1, no heat transfer through the surface, and validity of a linear temperature-viscosity relation, it is necessary only to solve the differential equations for two components of the vector potential.

In the limit of vanishing cone angle (finite angle of attack), the boundary-layer equations become precisely those governing the compressible flow over a yawed infinite cylinder of diameter equal to the local diameter of the cone at the point under consideration. The cross and spanwise flows are coupled through the density, however, and it is not proper to compute the cross flow by two-dimensional methods, as may be done in the incompressible case. This coupling depends on the stream Mach number and not on the Mach number of the cross flow.

In the limit of vanishing angle of attack (finite cone angle), the boundary-layer equations reduce to those governing flow about a cone at zero angle of attack. A sufficiently small angle of attack may be considered to impose small perturbations on the flow at zero angle of attack. If these perturbations are written in a form appropriate to the stream boundary conditions provided by the nonviscous perturbation theory, ordinary differential equations result. These may then be solved by numerical integration to obtain the fluid velocities and state quantities in the boundary layer. The type of perturbation method used in this report would be improper in the vicinity of any separation point of the basic flow. No such difficulty arises in the present application.

According to the perturbation analysis, the boundary-layer thickness associated with the cross (circumferential) velocity is constant around the body at a given distance from the apex. The shear associated with this cross flow gives rise to lift and moment on the body. No separation of the cross flow occurs, presumably as a consequence of the favorable circumferential pressure gradient.

Secondary flow occurs in the boundary layer of a cone at angle of attack; the slow fluid near the base of the boundary layer tends to incline more toward the direction of the circumferential pressure gradient then does the outer flow. This mechanism causes a concentration of low-energy air at the low-pressure side of the cone (top, for positive angle of attack). Therefore, taking into account the change in the profile of meridional velocity due to angle of attack, the boundary-layer thickness associated with this profile is greater at the top and less on the bottom of the cone than the value appropriate to the case of zero angle of attack. The reverse is true of meridional skin friction. Meridional skin friction is integrated to give the viscous drag of the cone. The effect of angle of attack on drag is second order in angle of attack and is ignored in the present analysis.

The changes in the meridional velocity profile due to angle of attack suggest that a decrease in laminar stability on the low-pressure side and the reverse effect on the high-pressure side might be expected.

Lewis Flight Propulsion Laboratory
National Advisory Committee for Aeronautics
Cleveland, Ohio, August 10, 1951

APPENDIX A

SYMBOLS

2286

The following symbols are used in this report:

A_1	related to perturbation in meridional velocity u outside boundary layer
A_2	related to perturbation in circumferential velocity outside boundary layer
A_3	related to perturbation in pressure outside boundary layer
A_4	related to perturbation in density outside boundary layer
C	constant of proportionality in temperature-viscosity relation
C_{D_v}	coefficient of viscous drag
C_{L_v}	coefficient of viscous lift
C_{m_v}	coefficient of viscous pitching moment
C_p	specific heat at constant pressure
D_v	viscous drag
f	component of vector potential related to meridional velocity u
f_0, f_1	value of f for $\alpha = 0$ and perturbation of f, respectively
g	component of vector potential related to circumferential velocity
g_1	linear approximation to g
h_1, h_2, h_3	functions composing f_1 and g_1

L_v	viscous lift
M	Mach number
m_v	viscous pitching moment about cone apex
p	pressure
R	Reynolds number, subscript indicates length upon which based
T	temperature
u, v, w	meridional, normal, and circumferential velocity component, respectively
x, y	coordinates taken along cone generators and normal to cone surface
α	angle of attack
γ	ratio of specific heats
δ	boundary-layer thickness
δ_x	displacement thickness associated with u-profile
δ_φ	displacement thickness associated with w-profile
ε	divergence between outer and limiting streamlines
ζ	dimensionless coordinate $(\varphi \sin \Theta)$
Θ, θ	semivertex angle of cone and sine of semivertex angle
λ	dimensionless coordinate $\left(\sqrt{3}\left[\left(\frac{p}{\bar{p}}\right)^{-\frac{1}{2}} \int_0^y \rho \, dy\right]_x^{-\frac{1}{2}}\right)$
μ	viscosity coefficient
ρ	density
φ	angular coordinate measured circumferentially around cone

Subscripts:

w	denotes evaluation at cone surface
0	denotes evaluation in undisturbed stream
1	denotes evaluation at outer edge of boundary layer

Subscript notation for partial differentiation is used.

Superscripts:

'	Primes denote ordinary differentiation.
–	Bars (as in $\bar{u}$ or $\bar{R}$) denote evaluation in nonviscous flow next to cone surface in case of zero angle of attack.

APPENDIX B

NUMERICAL DETERMINATION OF PROFILE FUNCTIONS

By L. Richard Turner

The four functions $f_0(\lambda)$, $h_1(\lambda)$, $h_2(\lambda)$, and $h_3(\lambda)$ have been obtained by numerical solution of the boundary-value problems set forth in equations (18) and (28) to (30).

Differential equation (18) is the basic Blasius equation; it has been solved to provide the values of the function $f_0(\lambda)$ required for the remaining integrations. Boundary conditions (21) are specified at two points $\lambda = 0,\infty$ and thus cannot be satisfied directly by a step-by-step integration process. This difficulty may be avoided as follows: Define

$$q(\sigma) \equiv af_0(\lambda)$$

$$\sigma \equiv \frac{1}{a}\lambda$$

where a is an arbitrary constant. Substitution into equations (18) and (21) yields

$$q\,q'' + 2q''' = 0 \tag{B1}$$

$$q'(\infty) = a^2 \qquad q'(0) = q(0) = 0 \tag{B2}$$

Differential equation (B1) may be integrated using the boundary conditions $q'(0) = q(0) = 0$ and an arbitrary value of $q''(0)$. A constant value of $q'(\sigma)$ will ultimately be reached and may be equated to a^2 since a^2 is arbitrary. The resulting value of a may then be used to invert the transformation leading to equations (B1) and (B2), thus determining the solution $f_0(\lambda)$.

Equations (28) to (30) are linear in their dependent variables; solutions that satisfy the boundary conditions at $\lambda = \infty$ may therefore be found by appropriate linear combinations of the complementary and particular solutions satisfying the given boundary conditions at the origin.

The functions h_1, h_2, and h_3 were found by computing the complementary and particular integrals of equations (28a) and (30a) subject to the following boundary conditions:

Equation	Integral	h(0), h'(0)	h"(0)
(28a)	Complementary	0	1/3
(28a)	Particular	0	1/3
(30a)	Complementary	0	1/3
(30a)	Particular	0	0

The values of $h''(0)$ are arbitrary.

The function h_1 is thus composed of the complementary and particular solutions of equation (28a), linearly combined in such a way that $h_1'(\infty) = 0$ (boundary condition (28b)). The function $h_2(\lambda)$ was obtained by scaling the complementary integral of equation (30a), which satisfies equation (29a), so that $h_1(\infty) = 1$ (boundary condition (29b)). The function $h_3(\lambda)$ is composed of the complementary and particular integrals of equation (30a), combined linearly so that $h_3'(\infty) = 0$ (boundary condition (30b)).

The four differential equations (18a) and (28a) to (30a) were integrated numerically by a method somewhat similar to that of Adams (see reference 11). Given the complete solution for the function in question at six equally spaced points, the solution may be extended to the next point as follows: A sixth-degree polynomial is passed through the six known and one unknown values of the third derivative. This polynomial may be integrated to give the value and first two derivatives of the function at the seventh point in terms of the unknown third derivative. Substitution of these results into the differential equation evaluated at the seventh point yields an algebraic equation for the third derivative at that point, which may be solved, thus extending the solution of the differential equation by one step. This process is repeated out to sufficiently large values of λ so that the boundary conditions at $\lambda = \infty$ may be satisfied to the desired degree of accuracy. A step size of 0.01 was used for equation (18a), and a step size of 0.02 was used for equations (28a) to (30a).

The use of this method requires that an initial set of values of each function and its first two derivatives be known in advance for the first six intervals, starting at the origin. These values were obtained by use of a method of successive approximation which is a numerical application of the classical Picard iteration process.

All the numerical integrations were performed on the IBM Card Programmed Electronic Calculator, and carried out to ten decimal places. The computations were checked by computing the third and seventh differences of the third derivatives to assure freedom from computational error and from significant truncation error, respectively.

REFERENCES

1. Stone, A. H.: On Supersonic Flow past a Slightly Yawing Cone. Jour. Math. and Phys., vol. XXVII, no. 1, April 1948, pp. 67-81.

2. Anon.: Tables of Supersonic Flow Around Cones. Tech. Rep. No. 1, Dept. Elec. Eng., M.I.T., 1947.

3. Anon.: Tables of Supersonic Flow around Yawing Cones. Tech. Rep. No. 3, Dept. Elec. Eng., M.I.T., 1947.

4. Ferri, Antonio: Supersonic Flow Around Circular Cones at Angles of Attack. NACA TN 2236, 1950.

5. Moore, Franklin K.: Three-Dimensional Compressible Laminar Boundary-Layer Flow. NACA TN 2279, 1951.

6. Hantsche and Wendt: The Laminar Boundary Layer on a Circular Cone at Zero Incidence in a Supersonic Stream. Rep. and Trans. No. 276, British M.A.P., Aug. 1946.

7. Allen, H. Julian: Pressure Distribution and Some Effects of Viscosity on Slender Inclined Bodies of Revolution. NACA TN 2044, 1950.

8. Van Dyke, Milton D.: First- and Second-Order Theory of Supersonic Flow Past Bodies of Revolution. Jour. Aero. Sci., vol. 18, no. 3, March 1951, pp. 161-178.

9. Sears, W. R.: The Boundary Layer of Yawed Cylinders. Jour. Aero. Sci., vol. 15, no. 1, Jan. 1948, pp. 49-52.

10. Chapman, Dean R., and Rubesin, Morris W.: Temperature and Velocity Profiles in the Compressible Laminar Boundary Layer with Arbitrary Distribution of Surface Temperature. Jour. Aero. Sci., vol. 16, no. 9, Sept. 1949, pp. 547-565.

11. Scarborough, James B.: Numerical Mathematical Analysis. Chap. 13. Johns Hopkins Press (Baltimore), 1st ed., 1930, pp. 267-273.

TABLE I - PROFILE FUNCTIONS

λ	f_0	f_0'	f_0''	h_1	h_1'	h_1''	h_2	h_2'	h_2''	h_3	h_3'	h_3''
0	0	0	0.332058	0	0	0.428803	0	0	0.498724	0	0	-0.031614
.2	.006841	.066408	.331984	.008152	.079100	.382269	.009974	.099734	.498504	-.000632	-.008321	-.031570
.4	.026560	.132784	.331470	.030757	.144963	.296564	.039864	.199313	.498880	-.002526	-.012615	-.031270
.6	.059735	.198937	.330080	.065251	.197841	.252589	.089663	.298343	.492791	-.005671	-.016810	-.030488
.8	.106108	.264709	.327390	.109057	.238178	.171304	.159142	.396172	.484754	-.010035	-.024784	-.029042
1.0	.165572	.329780	.323007	.159728	.288608	.113699	.247993	.491912	.471737	-.015582	-.030421	-.026801
1.2	.237948	.393777	.316590	.214962	.283988	.060745	.355895	.584474	.452846	-.022185	-.035525	-.023700
1.4	.322982	.456282	.307868	.272648	.291277	.013341	.481488	.672619	.427508	-.029721	-.039954	-.019750
1.6	.420322	.516757	.295564	.330882	.289726	-.027745	.624360	.755035	.395555	-.038075	-.043485	-.015043
1.8	.528519	.574769	.282931	.388032	.280639	-.081937	.785035	.830421	.357320	-.047041	-.046039	-.009752
2.0	.650028	.629766	.266752	.442729	.265433	-.088699	.955981	.897599	.313651	-.056410	-.047602	-.004120
2.2	.781196	.681311	.248351	.493895	.245566	-.108574	1.141481	.955609	.265901	-.065957	-.047827	.001583
2.4	.922293	.728983	.228092	.540741	.222474	-.121198	1.337589	1.003605	.215840	-.075457	-.047034	.008985
2.6	1.072509	.772456	.206455	.582781	.197523	-.127290	1.542310	1.041927	.165514	-.084693	-.045201	.011845
2.8	1.230981	.811510	.184007	.619708	.171943	-.127617	1.755678	1.070135	.117055	-.093470	-.042463	.015887
3.0	1.396812	.846045	.161360	.651567	.146787	-.123157	1.969741	1.089006	.072455	-.101625	-.039002	.018928
3.2	1.569100	.876082	.139128	.678515	.122958	-.114921	2.188720	1.099487	.033595	-.109033	-.035028	.020872
3.4	1.746955	.901762	.117876	.700871	.101003	-.104075	2.409058	1.102814	.001068	-.115814	-.030762	.021720
3.6	1.928551	.923350	.098086	.719071	.081412	-.091663	2.629453	1.100400	-.023950	-.121331	-.026417	.021559
3.8	2.116036	.941118	.080128	.733807	.064379	-.078834	2.848934	1.093726	-.041605	-.125189	-.022194	.020644
4.0	2.305753	.955619	.064234	.744997	.049948	-.065778	3.066784	1.084216	-.052413	-.130227	-.018243	.018877
4.2	2.498046	.966957	.050520	.753753	.038015	-.053705	3.282517	1.073156	-.057291	-.133512	-.014673	.016775
4.4	2.692588	.975871	.038972	.760356	.028586	-.042819	3.495995	1.061617	-.057405	-.136126	-.011648	.014450
4.6	2.888255	.982684	.029484	.765242	.020792	-.033560	3.707188	1.050426	-.054024	-.138163	-.008895	.012085
4.8	3.085528	.987780	.021871	.768789	.014940	-.025407	3.916227	1.040169	-.048370	-.139715	-.006706	.009829
5.0	3.283281	.991542	.015907	.771315	.010331	-.018922	4.123338	1.031158	-.041521	-.140874	-.004949	.007780
5.2	3.481875	.994246	.011342	.773079	.007282	-.013785	4.328785	1.023572	-.034339	-.141721	-.003576	.006000
5.4	3.680927	.996156	.007928	.774288	.004959	-.009825	4.532860	1.017401	-.027458	-.142326	-.002550	.004511
5.6	3.880298	.997478	.005432	.775100	.003286	-.006864	4.735833	1.012542	-.021275	-.142750	-.001753	.003308
5.8	4.079890	.998376	.003648	.775636	.002144	-.004660	4.937953	1.008850	-.016008	-.143042	-.001189	.002369
6.0	4.279629	.998973	.002402	.775982	.001372	-.003128	5.139429	1.006075	-.011707	-.143237	-.000780	.001856
6.2	4.479485	.999363	.001550	.776202	.000881	-.002047	5.340434	1.004086	-.008334	-.143368	-.000514	.001151
6.4	4.679385	.999612	.000981	.776339	.000530	-.001312	5.541103	1.002687	-.005779	-.143449	-.000328	.000785
6.6	4.879304	.999768	.000608	.776422	.000320	-.000823	5.741538	1.001729	-.003906	-.143501	-.000205	.000493
6.8	5.079288	.999864	.000370	.776472	.000190	-.000506	5.941815	1.001088	-.002576	-.143534	-.000125	.000314
7.0	5.279247	.999922	.000220	.776502	.000110	-.000305	6.141988	1.000670	-.001666	-.143553	-.000075	.000196
7.2	5.479235	.999956	.000129	.776518	.000063	-.000180	6.342095	1.000403	-.001048	-.143565	-.000044	.000120
7.4	5.679228	.999978	.000074	.776528	.000035	-.000104	6.542168	1.000237	-.000641	-.143572	-.000025	.000072
7.6	5.879225	.999987	.000041	.776533	.000019	-.000059	6.742182	1.000137	-.000384	-.143576	-.000014	.000042
7.8	6.079223	.999993	.000023	.776536	.000010	-.000033	6.942215	1.000077	-.000225	-.143578	-.000008	.000024
8.0	6.279222	.999996	.000012	.776538	.000005	-.000018	7.142225	1.000043	-.000129	-.143579	-.000004	.000013
8.2	6.479221	.999998	.000006	.776538	.000003	-.000009	7.342251	1.000023	-.000072	-.143580	-.000002	.000007
8.4	6.879221	.999999	.000003	.776539	.000001	-.000005	7.542254	1.000012	-.000039	-.143580	-.000001	.000004
8.6	6.879221	1.000000	.000002	.776539	.000001	-.000002	7.742256	1.000006	-.000021	-.143580	-.000001	.000002
8.8	7.079221	1.000000	.000001	.776539	0	-.000001	7.942257	1.000003	-.000011	-.143580	0	.000001
9.0	7.279221	1.000000	0	.776539	0	-.000001	8.142258	1.000002	-.000006	-.143580	0	.000001
9.2	7.479221	1.000000	0	.776539	0	-0	8.342258	1.000001	-.000003	-.143580	0	0

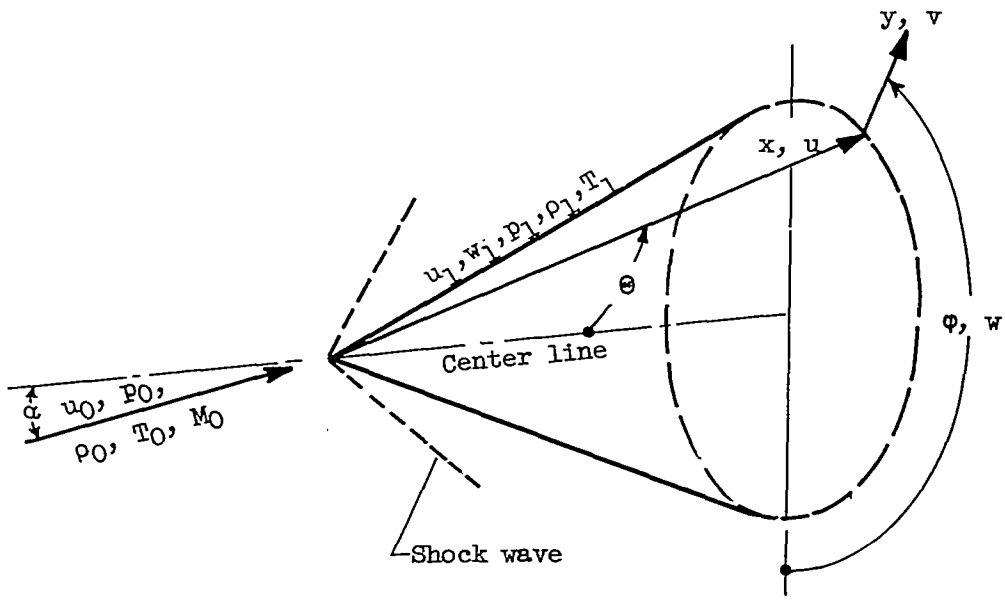

Figure 1. - Notation for cone at angle of attack in supersonic stream.

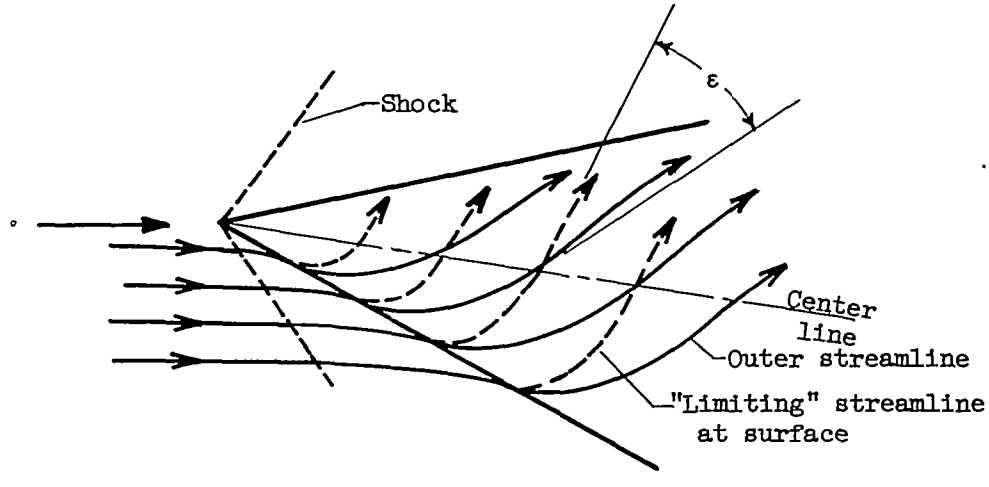

Figure 2. - Streamline patterns illustrating "secondary flow."

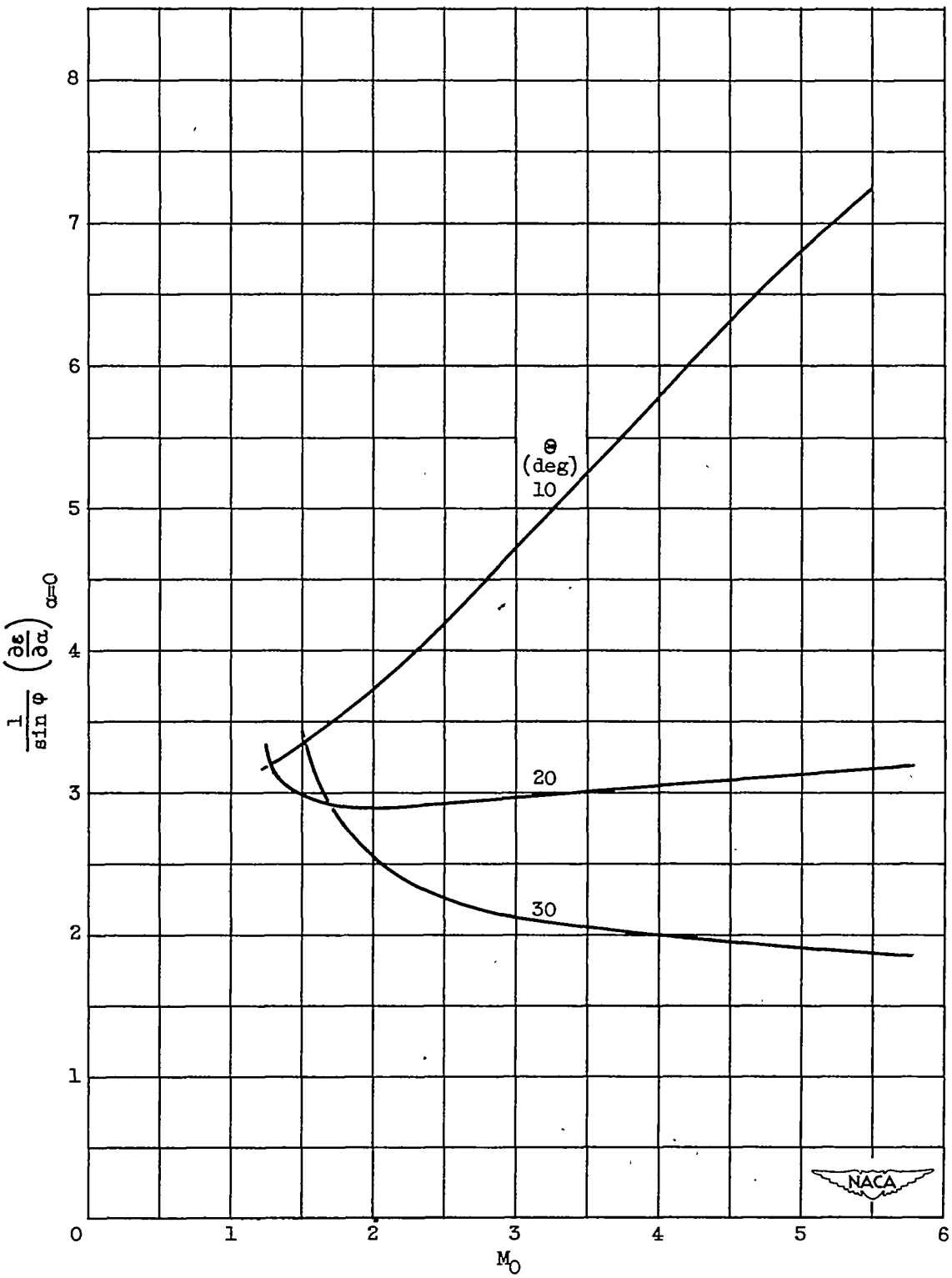

Figure 3. - Streamline divergence across boundary layer.

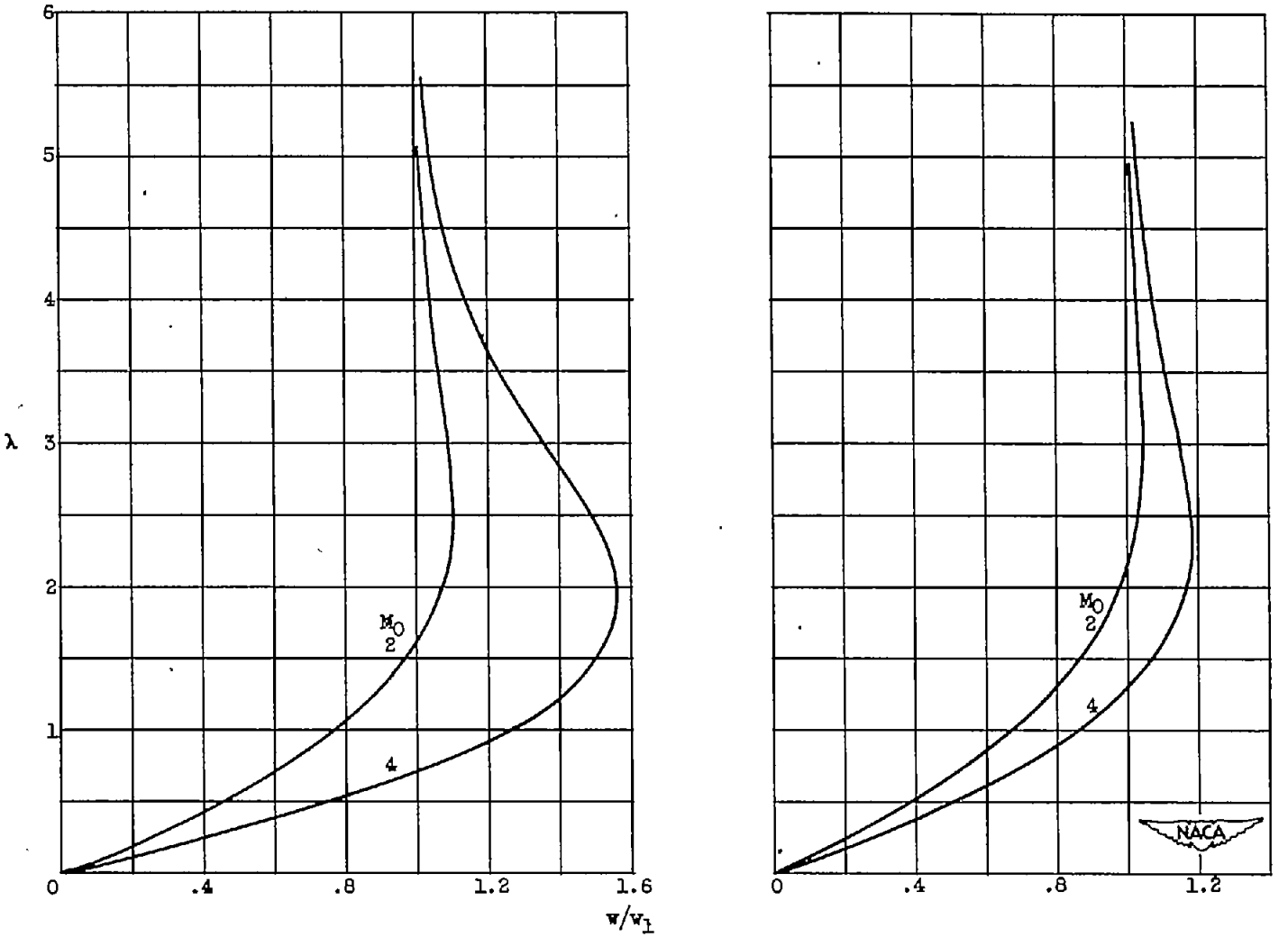

(a) Semivertex angle, 10°.

(b) Semivertex angle, 30°.

Figure 4. - Profile of circumferential velocity component.

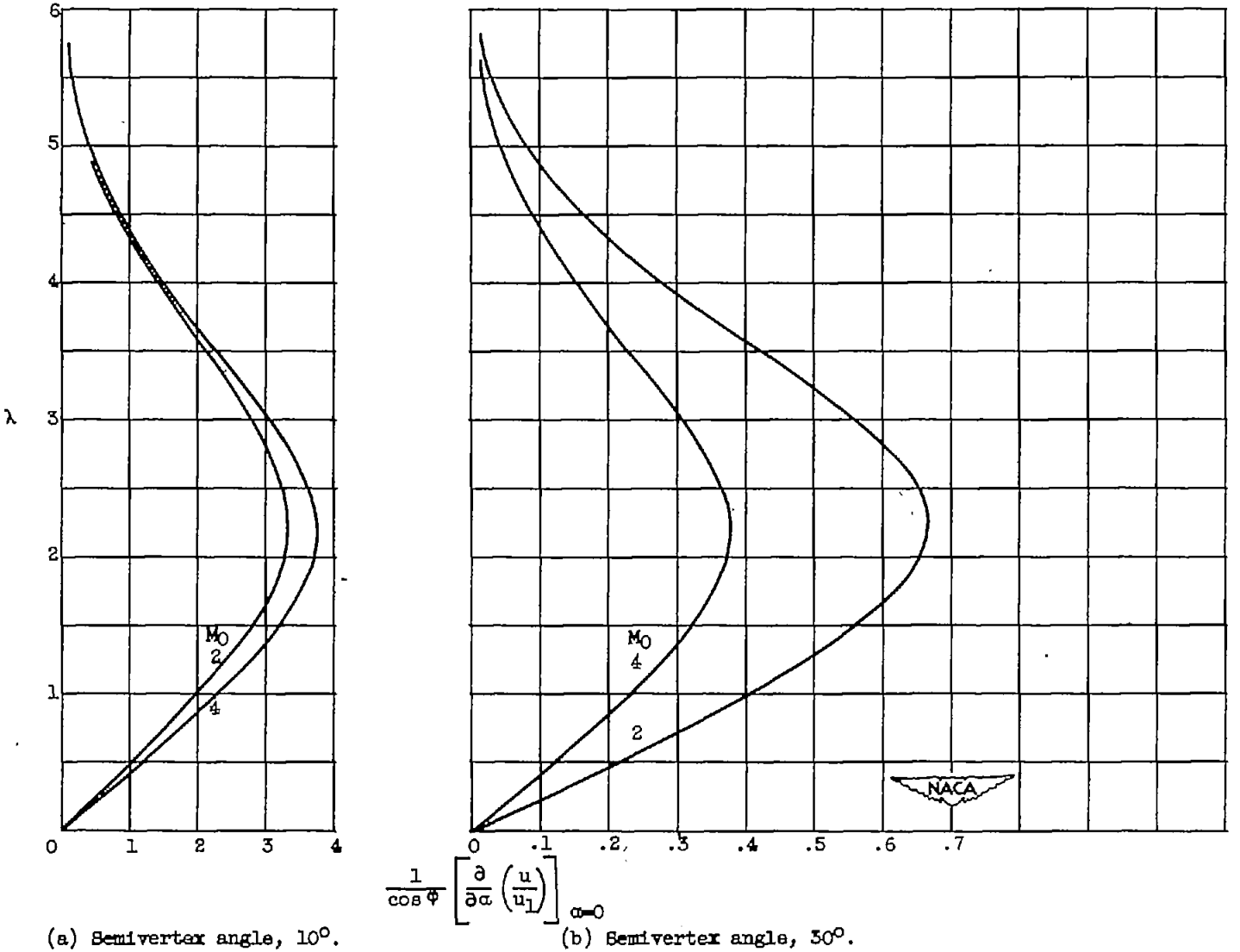

(a) Semivertex angle, 10°. (b) Semivertex angle, 30°.

Figure 5. - Increment in meridional profile due to angle of attack.

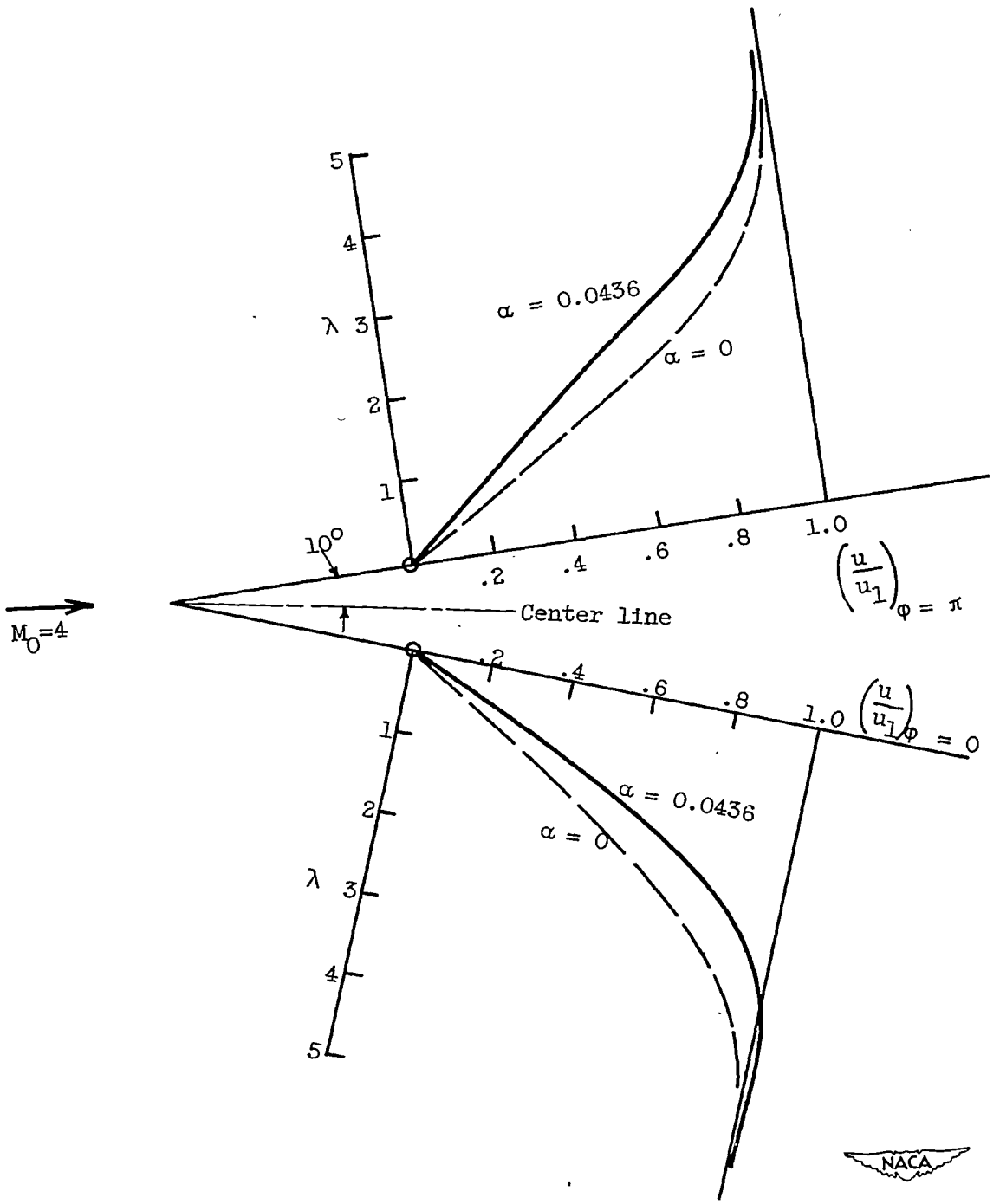

Figure 6. - Profiles of meridional velocity component in plane $\varphi = 0, \pi$. Semivertex angle, 10°; free-stream Mach number, 4; angle of attack, 0.0436 (= 2.5°).

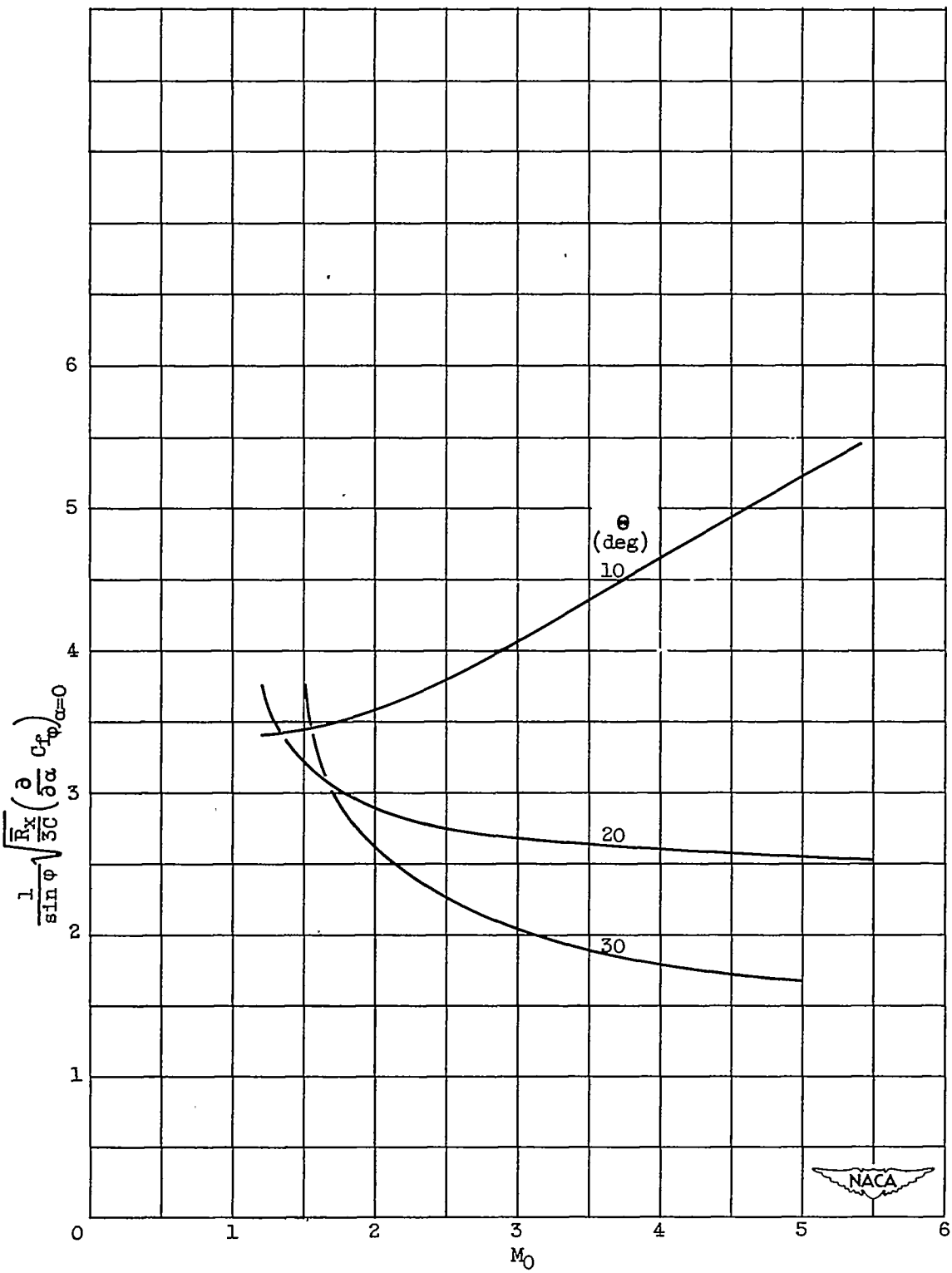

Figure 7. - Circumferential skin friction due to angle of attack.

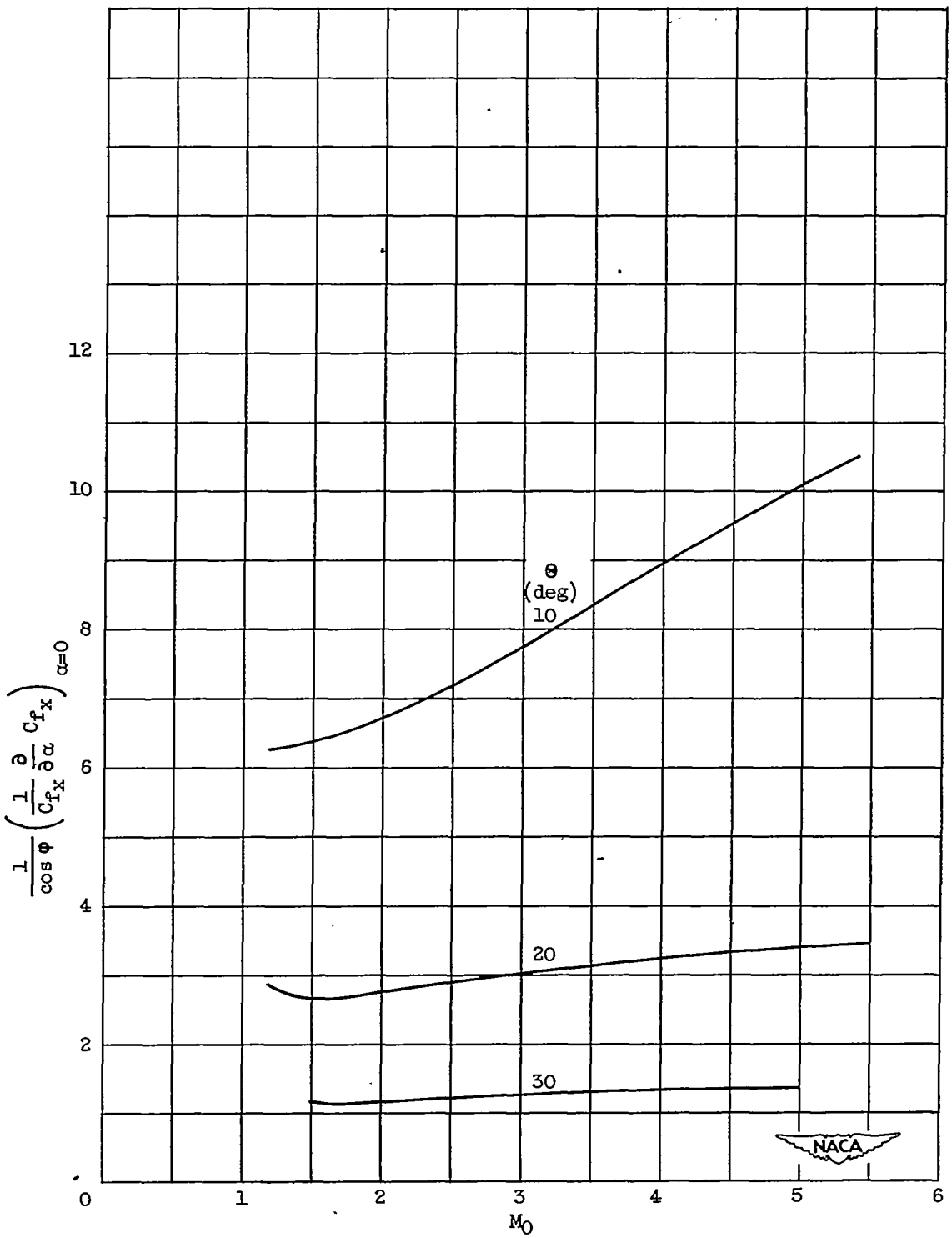

Figure 8. - Increment in meridional skin friction due to angle of attack.

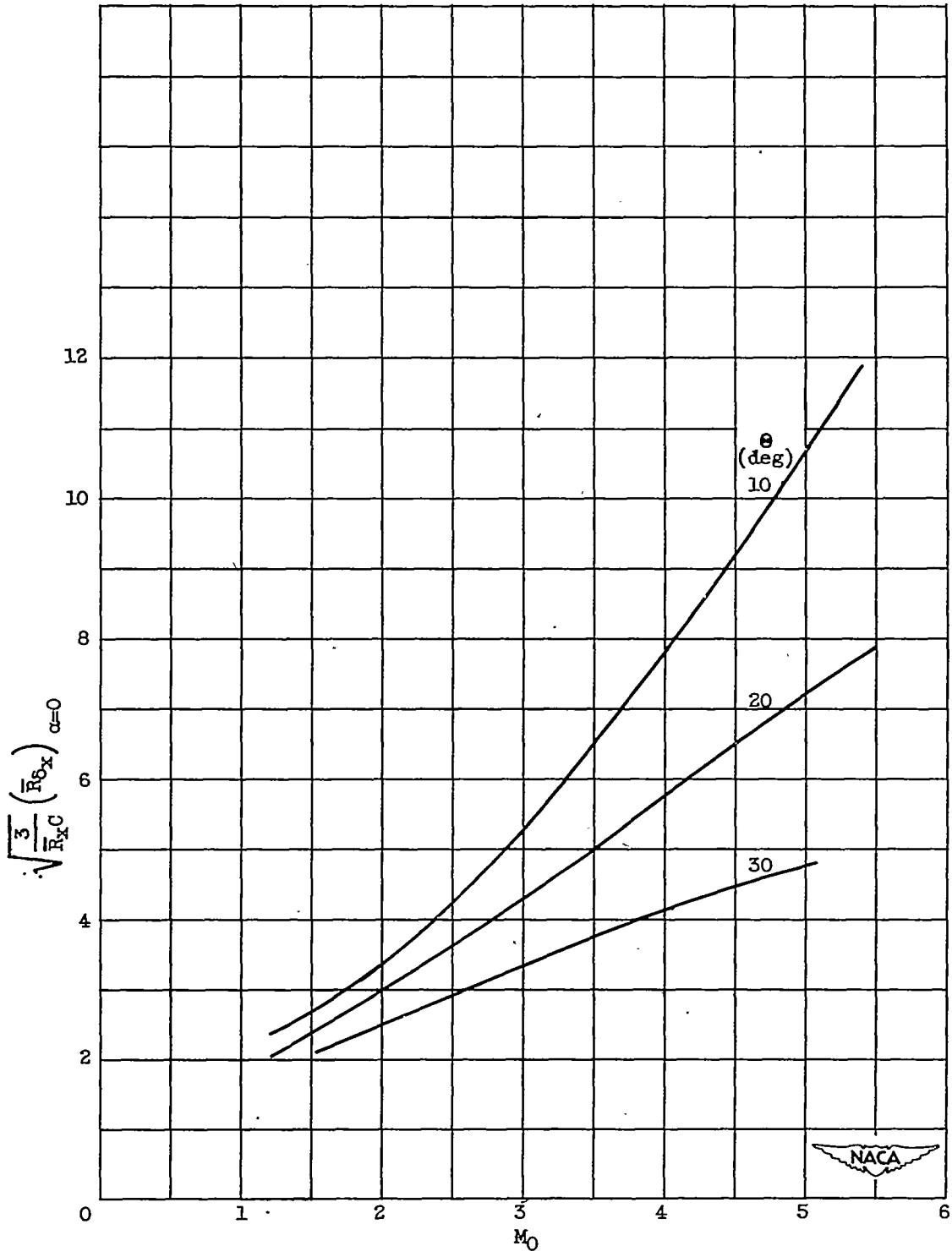

Figure 9. - Displacement thickness of meridional velocity profile at zero angle of attack.

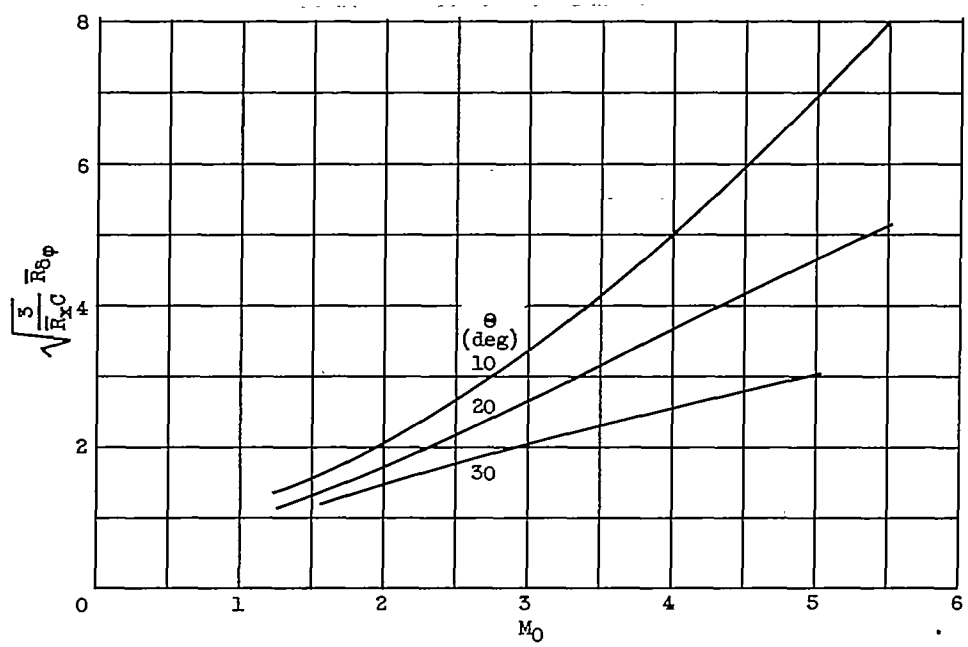

Figure 10. - Displacement thickness of circumferential velocity profile due to angle of attack.

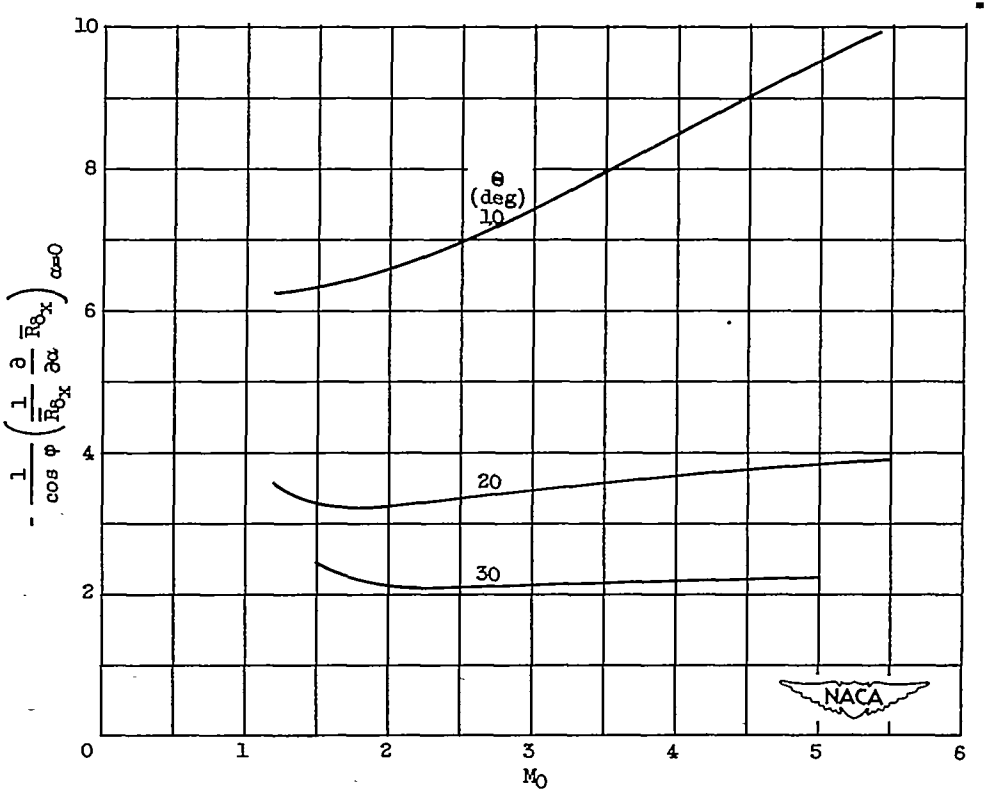

Figure 11. - Increment in displacement thickness of meridional velocity profile due to angle of attack.

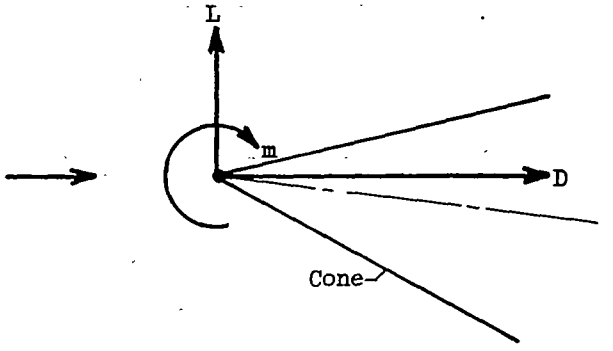

Figure 12. - Conventions for aerodynamic forces and moments on cone.

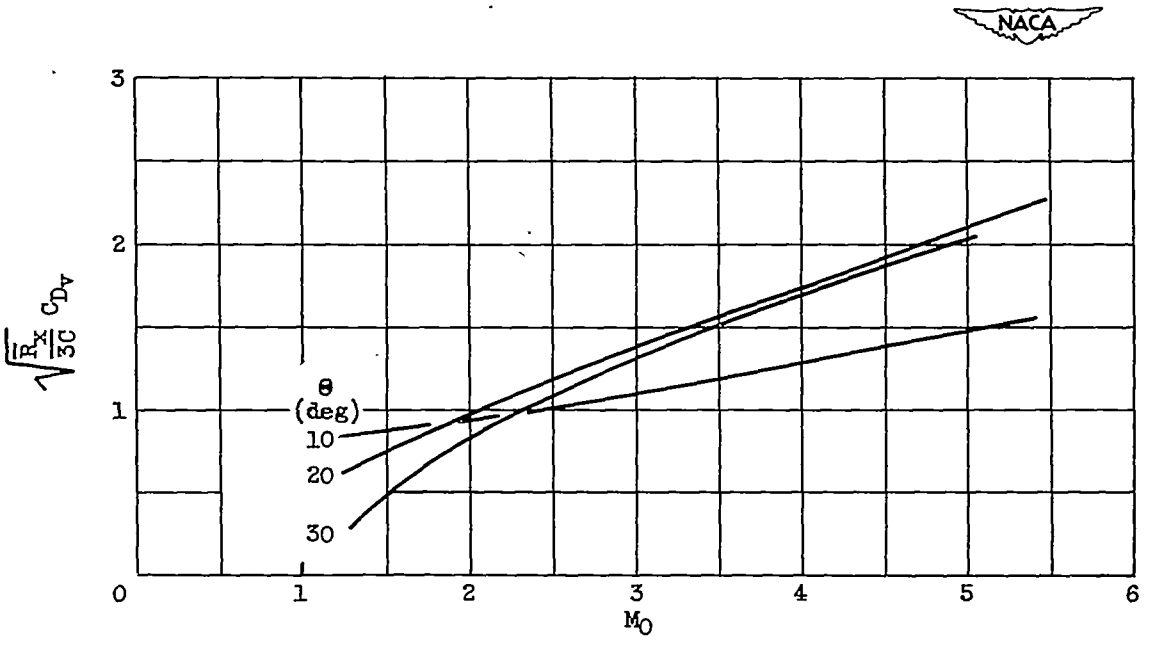

Figure 13. - Coefficient of viscous drag.

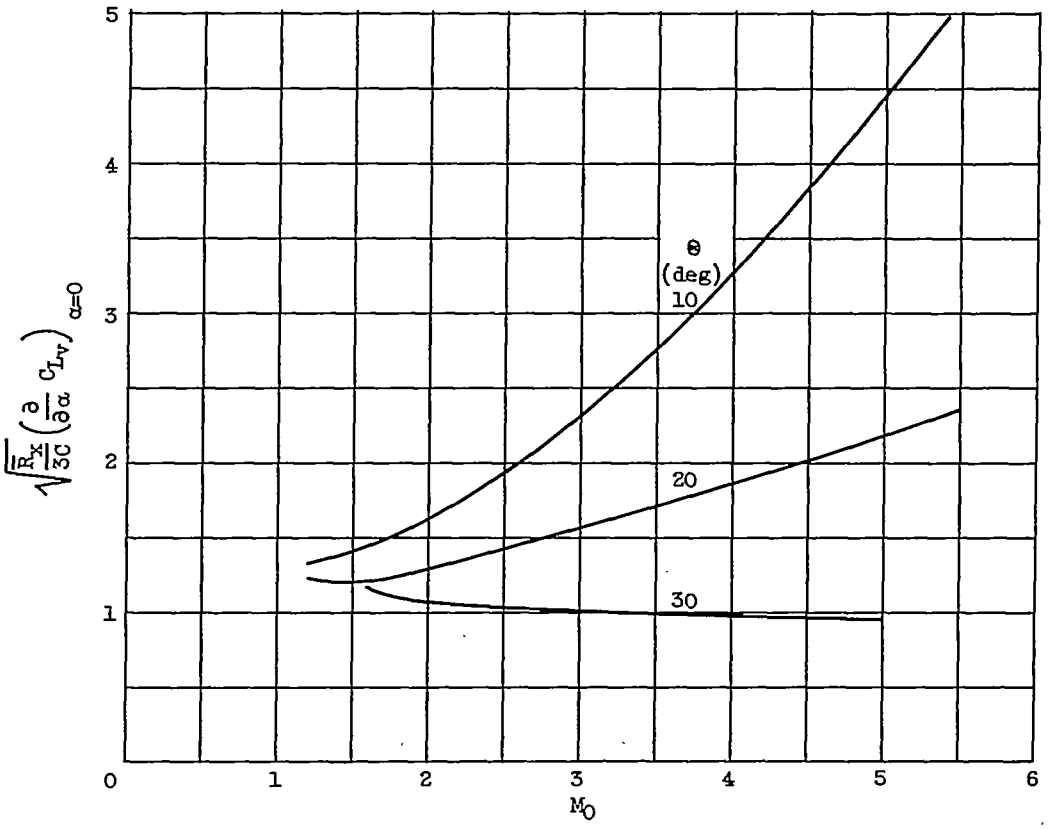

Figure 14. - Coefficient of viscous lift.

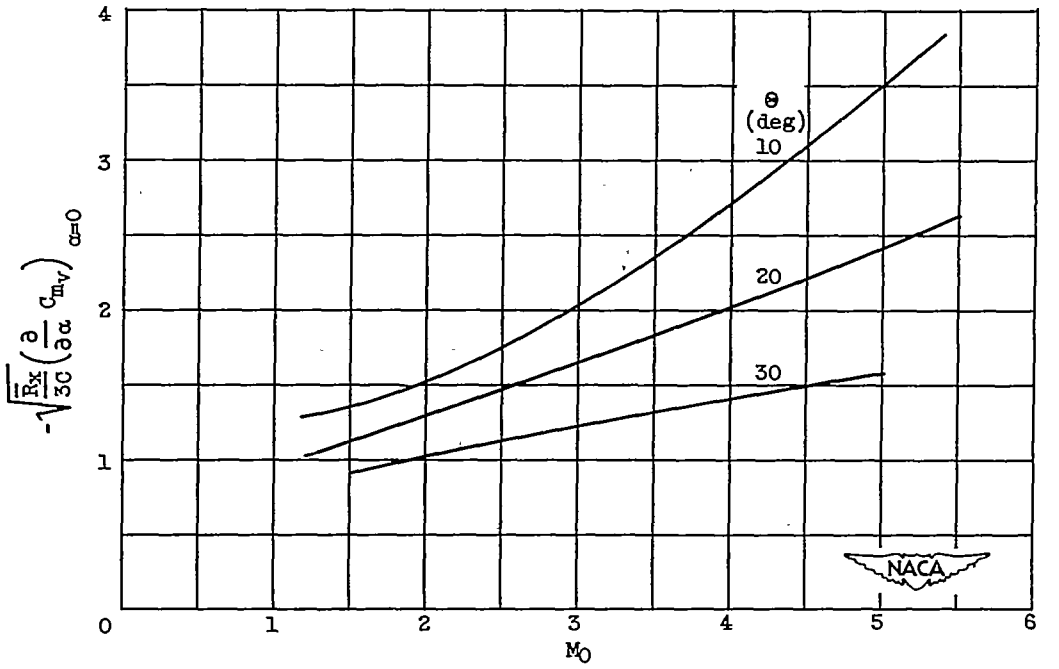

Figure 15. - Coefficient of viscous pitching moment about cone apex.

NACA-Langley - 10-18-51 - 1000